Zooplankton community succession and trophic links during a mesocosm experiment in the coastal upwelling off Callao Bay (Peru)

Patricia Ayón Dejo[1], Elda Luz Pinedo Arteaga[1], Anna Schukat[2], Jan Taucher[3], Rainer Kiko[3,4], Helena Hauss[3,5], Sabrina Dorschner[2], Wilhelm Hagen[2], Mariona Segura-Noguera[6], and Silke Lischka[3,5]

[1]Instituto del Mar del Perú (IMARPE), Dirección General de Investigaciones en Oceanografía y Cambio Climático, Callao, Perú
[2]University of Bremen, BreMarE Bremen Marine Ecology, Marine Zoology, Bremen, Germany
[3]GEOMAR Helmholtz Centre for Ocean Research Kiel, Biological Oceanography, Kiel, Germany
[4]Laboratoire d'Océanographie de Villefranche-sur-Mer, Sorbonne Université, Villefranche-sur-Mer, France
[5]Department of Computer Science, Christian Albrechts University Kiel, Kiel, Germany
[6]Institut de Ciències del Mar (ICM_CSIC), Barcelona, Spain

Correspondence: Silke Lischka (slischka@geomar.de)

Abstract.

The Humboldt Current Upwelling System (HUC) is the most productive eastern boundary upwelling system (EBUS) in terms of fisheries yield on the planet. EBUS are considered hotspots of climate change with predicted expansion of mesopelagic oxygen minimum zones (OMZs) and related changes in frequency and intensity of upwelling of nutrient-rich/oxygen-low deep-water. To increase our mechanistic understanding of how upwelling impacts plankton communities and trophic links, we investigated mesozooplankton community succession and gut fluorescence, fatty acid and elemental compositions (C, N, O, P), and stable isotope (δ^{13}C, δ^{15}N) ratios of dominant meso- and microzooplankton representatives in a mesocosm setup off Callao (Peru) after simulated upwelling with OMZ water from two different locations and different N:P signatures (moderate and extreme treatments). An oxycline between 5 and 15 m with hypoxic conditions (<50 μL^{-1}) below ~10 m persisted in the mesocosms throughout the experiment. No treatment effects were determined for the measured parameters but differences in nutrient concentrations established through OMZ water additions were only minor. Copepods and polychaete larvae dominated in terms of abundance and biomass. Development and reproduction of the dominant copepod genera *Paracalanus* sp., *Hemicyclops* sp., *Acartia* sp., and *Oncaea* sp. were hindered as evident from accumulation of adult copepodids but largely missing nauplii. Failed hatching of nauplii in the hypoxic bottom layer of the mesocosms and poor nutritional condition of copepods suggested from very low gut fluorescence and fatty acid compositions most likely explains the retarded copepod development. Correlation analysis revealed no particular trophic relations between dominant copepods and phytoplankton groups. Possibly particulate organic matter with relatively high C:N ratio was a major diet of copepods. C:N ratios of copepods and polychaetes ranged between 4.8–5.8 and 4.2–4.3, respectively. δ^{15}N was comparatively high (~13–17‰) potentially because the injected OMZ source water was enriched in δ^{15}N as a result of anoxic conditions. Elemental ratios of dinoflagellates deviated strongly from the Redfield ratio. We conclude opportunistic feeding of copepods may have played an important role in the pelagic food web. Overall, projected changes in frequency and intensity of upwelling hypoxic waters may make a huge difference for copepod reproduction and may be further enhanced by varying N:P ratios of upwelled OMZ water masses.

1 Introduction

The Humboldt Current System (HCS) is the most productive eastern boundary upwelling system (EBUS) in terms of fisheries yield despite only moderate primary production rates compared with the other three major EBUS (Bakun and Weeks, 2008; Chavez et al., 2008). About 10 % of global fish landings originate in the HCS due to wind-driven upwelling of cold nutrient-rich waters to the sunlit surface (Chavez et al., 2008). Such extraordinary high fisheries yield, especially off Peru, results from a high trophic transfer efficiency compared to the other EBUS (Chavez and Messié, 2009).

Zooplankton play the key role in transfering biomass from primary producers to pelagic fishes (Ayón et al., 2008b, 2011). Particularly, upwelling and consequent productivity dynamics are tightly coupled in the northern HCS, as indicated by the strong bottom-up driven control of Peruvian anchovy (*Engraulis ringens*), the most important exploited planktivorous fish in the region. Accordingly, changes in zooplankton biomass and composition have direct consequences for higher trophic levels, e.g. fish, seabirds and marine mammals (Ayón et al., 2008b, 2011; Aronés et al., 2019).

The HCS is characterized by a pronounced shallow and intense (acidic) oxygen minimum zone (OMZ) (Bakun and Weeks, 2008), where hypoxic waters can approach the surface (<10 m depth, Graco et al. (2017); Bach et al. (2020)). Also, the HCS is characterized by massive loss and source processes of dissolved inorganic nitrogen (N) and phosphorus (P), respectively (Ingall and Jahnke, 1994; Kalvelage et al., 2011), so that water masses with N:P ratios substantially below the canonical Redfield ratio are upwelled into the surface layer (Franz et al., 2012a; Löscher et al., 2016). Such upwelled water masses have major impacts on total phytoplankton biomass (Franz et al., 2012b), community structure, and fatty acid composition (Hauss et al., 2012), with unclear consequences for consumers. The OMZ will further expand and intensify in the course of global climate change, with severe implications for biogeochemical cycles and pelagic life (Stramma et al., 2008; Schmidtko et al., 2017).

On the continental shelf, the zooplankton community in the Peruvian upwelling region is dominated by small herbivorous copepods that consume phytoplankton blooms in the freshly upwelled waters (Espinoza and Bertrand, 2014). As primary production decreases with distance from shore, the continental slope and oceanic zooplankton communities typically become dominated by euryphagous or carnivorous organisms such as large copepods, euphausiids and gelatinous plankton (Ayón et al., 2008a). This large zooplankton, especially euphausiids, provides rich feeding grounds for Peruvian anchovy off the shelf, whereas on the shelf towards the coast, the contribution of copepods in their diet increases (Schwartzlose et al., 1999; Espinoza and Bertrand, 2008; Espinoza et al., 2009; Aronés et al., 2019).

The fertilizing effect of wind-driven upwelling of nutrient-rich waters in the HCS is subject to interannual variations due to El Niño events that weaken trade winds and increase flow of warm water into the eastern equatorial Pacific, hindering upwelling of nutrient-rich deeper water (Karl et al., 1995; Escribano, 1998; Carr, 2001). Also, upwelling intensities of nutrient-rich waters are not directly correlated with primary and secondary production off Peru: intermediate-strength upwelling favours high zooplankton abundance and biomass particularly in spring (October/November), while too strong or too weak upwelling hampers zooplankton productivity in winter and summer, respectively (Ayón et al., 2008a; Chavez and Messié, 2009; Aronés et al., 2019). Whether climate change will cause wind and, hence, upwelling intensities and patterns in the Pacific to decline

or increase is currently not clear (Bakun and Weeks, 2008; Gruber et al., 2012), but wind, and thus upwelling, in the poleward portions of EBUS have intensified and this trend is expected to continue (García-Reyes et al., 2015).

High fish production has been attributed to pelagic fish feeding directly on phytoplankton, suggesting high trophic transfer efficiency (Ryther, 1969; Walsh, 1981). More recent studies revealed the dominance of mostly large zooplankton (copepods and euphausiids) in the diet of anchovies (Konchina, 1991; Espinoza and Bertrand, 2008, 2014), and of smaller copepods, less euphausiids (compared to anchovies) and potentially also some phytoplankton in the diet of Pacific sardine (Espinoza et al., 2009). Such findings emphasize the key role of zooplankton in the pelagic food web off Peru, and Espinoza and Bertrand (2008) hypothesize a more efficient use of of primary production by zooplankton in the HCS than in other EBUS facilitating the high fish production.

Zooplankton species composition and biomass off Peru vary strongly on short time scales due to advection, peaks of larval production, trophic interactions, and community succession (Ayón et al., 2008a). Zooplankton composition itself is regulated by food quality and composition. Times of low primary production favour euryphagous or carnivorous over herbivorous zoo-plankton (Ayón et al., 2008a). In fact, micro- and mesozooplankton seem to control phytoplankton standing stocks over the shelf (Minas et al., 1986; Cullen et al., 1992; Franz et al., 2012a).

We conducted a large-scale *in situ* mesocosm experiment in the coastal Peruvian upwelling region off Callao, Peru, in austral summer 2017 to investigate impacts of upwelling on pelagic biogeochemistry, plankton communities, and food web dynamics. We simulated upwelling events by adding two different types of OMZ waters with different N:P signatures to each of four mesocosms. However, bioavailable inorganic nitrogen (N) concentrations in the collected OMZ source water were lower than expected. Due to this reason, the N difference established through the addition of OMZ water in the mesocosm treatments with a moderate and an extreme N:P signature (2.89 and 1.49, respectively) was only minor (2.2 μmol L^{-1}) but significant directly after the additions (Bach et al., 2020). Initially, diatoms dominated the phytoplankton communities in the mesocosms. After OMZ deep-water addition and concurrent exhaustion of N, the communities shifted towards a pronounced dominance of the mixotrophic dinoflagellate *Akashiwo sanguinea*. Initially ranging between 1.4 and 4.9 μg L^{-1} in the mesocosms, chlorophyll *a* increased only slightly after OMZ water addition to average mesocosm-specific concentrations of max. 5.6 μg L^{-1} between Day 12 and Day 40 without any pronounced peak or treatment separation. Only towards the end of the experiment (after Day 40), eutrophication due to defecating seabirds (guanotrophication) led to an intense phytoplankton bloom and concurrent increase of chlorophyll *a* to values around 20 μg L^{-1} in most mesocosms.

The goal of the present work was to study the mesozooplankton (MeZP) community response to the stimulated upwelling events and to investigate trophic links in OMZ influenced waters. Our hypotheses were: 1) The efficient utilization of a phy-toplankton bloom stimulated through upwelled deep waters by MeZP is higher at higher N:P stoichiometry (the moderate OMZ treatment) of upwelled water masses. To address this, we measured gut fluorescence and fatty acid compositions of dominant copepods to study whether feeding rates and contributions of biomarker fatty acids (Dalsgaard et al., 2003) increased differently at the two treatment levels. 2) The added OMZ water mass with the higher N:P stoichiometry would lead to higher zooplankton abundance and biomass compared to those with lower N:P (the extreme OMZ treatment). This was addressed by monitoring the temporal development (abundance, biomass) of the MeZP community in the mesocosms over the 50 d experi-

ment duration. Furthermore, correlation analysis of dominant copepod species with phytoplankton simultaneously monitored by project collaborators (Bach et al. 2020, Bernales et al. in prep.) was performed to gain insight into food web relations, and background information on the stable isotope (SI) and elemental composition (C:N) of dominant zooplankton taxa is provided. Concomitantly, we monitored the MeZP in the adjacent Pacific shelf waters at one sampling point nearby the mesocosm field to gain insight into the in situ zooplankton community development.

2 Methods

2.1 Experimental design

A detailed description of the mesocosm setup and the experimental manipulation is given in Bach et al. (2020). Briefly, eight KOSMOS mesocosm units (cylindrical 18.7 m long polyurethane bags, 2 m diameter, 54.4 $\pm$1.3 m^3 volume) were deployed on February 23, 2017, close to San Lorenzo Island about 6 km off Callao (12.0555° S, 77.2348° W, Fig.1). Nets (mesh size 3 mm) attached to both ends of the bags prevented larger plankton or nekton from entering the mesocosms during deployment. These meshes were removed as soon as the mesocosms were closed at the bottom with the sediment trap and the bags lifted above the surface, i.e. when the experiment started. On February 25 (defined as Day 0), the mesocosms were closed at the bottom with a sediment trap. To simulate upwelling with differing inorganic N:P ratios (i.e. with an extreme and a moderate OMZ signature), water was collected on Day 5 at station (hereafter St.) 1 from 30 m depth (12.03° S; 77.22° W) and on Day 10 at St. 3 from 70 m depth (12.04° S; 77.38° W) of the Instituto del Mar del Perú (IMARPE) time-series transect (Graco et al., 2017), using the 100 m^3 deep-water collectors described by Taucher et al. (2017). In each mesocosm $\sim$20 m^3 of water were exchanged with deep water from St. 3 (moderate OMZ signature: mesocosms M2, M3, M6, M7) or St. 1 (extreme OMZ signature: M1, M4, M5, M8). Deep water was injected on Day 11 and Day 12 to similar depth ranges as water had been removed from each mesocosm before (14–17 m and 1–9 m).

Oxygen minimum zones may reach very close to the surface (<10 m) in the near-coast region off Peru (Graco et al., 2017). To conserve the low O$_2$ bottom layer in the mesocoms that had established after the addition of low oxygen deep-water over the entire experimental duration, water column stratification was artificially maintained by evenly injecting a concentrated NaCl brine solution into the bottom layers of each mesocosm on Day 13 and Day 33. Otherwise, convective mixing induced through heat exchange with the surrounding Pacific would have destroyed the oxygen minimum layer in the mesocosms. For more details on the exact procedure of water exchange and deep-water injection as well as addition of the brine solution see Bach et al. (2020). According to these authors the mesocosm experiment was subdivided into three main phases based on the phytoplankton development: Phase 1 lasted from Day 1 until the OMZ water addition (Day 11/12) and was characterized by a diatom-dominated phytoplankton community, phase 2 started with the OMZ water addition until Day 40 and was characterized by a bloom of the mixotrophic dinoflagellate *Akashiwo sanguinea*, and phase 3 continued from Day 40 until the end of the experiment, when eutrophication by defecating seabirds (guanotrophication) triggered a late phytoplankton bloom in most mesocosms.
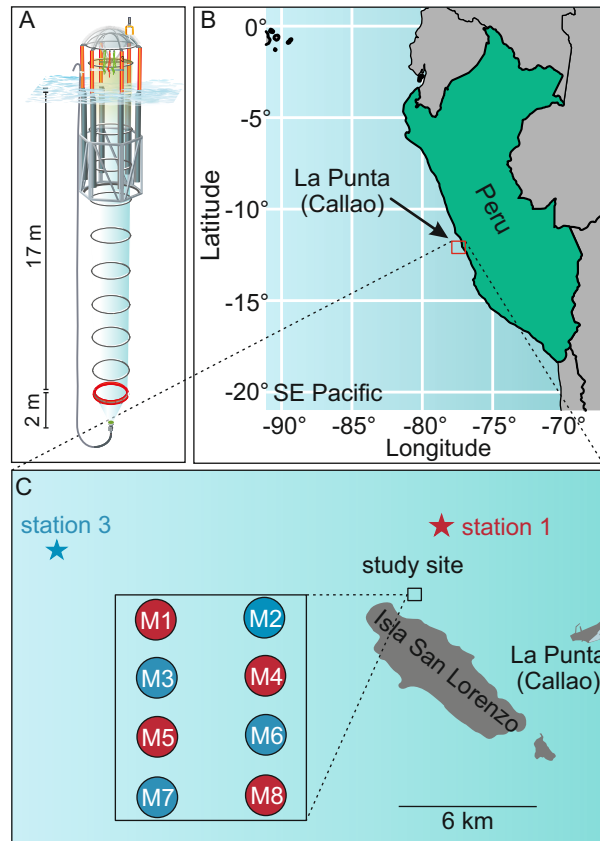
Figure 1. Study site of the mesocosm experiment. (a) One KOSMOS mesocosm unit with dimensions of the polyurthane bag and of the sediment trap. We acknowledge reprint permission of parts of this graphic from the AGU (Bach et al., 2016). (b) Location of the study region off La Punta (Callao). IMARPE and the laboratories for sample processing were located in La Punta (Callao). (c) Enlarged map of the study site that was located at the northern end of San Lorenzo Island. The additional square shows the mesocosm setup. OMZ water masses were collected at the IMARPE permanent stations 1 and 3 indicated by the stars. This figure is a reprint of Bach et al. (2020).

2.2 Zooplankton sampling

Mesozooplankton (MeZP) samples were always obtained with an Apstein net of 17 cm opening diameter equipped with a
100 μm net bag. Integrated vertical hauls were taken from 17 m depth of each mesocosm and the Pacific close to the mesocosm field. Due to technical/logistic constraints, regular sampling was not possible before Day 18. Therefore, sampling intervals varied between 2 and 7 days until Day 18. From then onwards, sampling was performed every 6 days. In total, two net hauls from each mesocosm and the Pacific were collected on ten sampling days (Day 0, 8, 10, 13, 18, 24, 30, 36, 42, 48). Contents from one net of each mesocosm were used for species abundance/biomass determination and contents from the other were used for picking live organisms for fatty acid and elemental analyses (C, N, P, δ^{13}C, δ^{15}N). Mesozooplankton was sampled in the afternoon between 13:00 and 17:00 (local time). As soon as the abundance net haul was retrieved onboard, the zooplankton

sample was emptied into sample bottles with filtered seawater (100 μm) and the net and cod end were subsequently rinsed to also wash zooplankton attached to the mesh into the sample bottle. The second net for live organisms was carefully poured into 5 L sampling containers prefilled with 4 L filtered seawater of ambient temperature to accommodate zooplankton organisms and reduce stress. All net samples were stored in cooling boxes to prevent heating until returning to the laboratory and further processing.

Microzooplankton samples for elemental composition analysis (detailed in section 2.8) were collected from integrated water samplers (see detailed description of water samplers in Bach et al. (2020)). In total, samples were taken at 12 sampling days (Day 0, 8, 10, 13, 16, 18, 20, 26, 30, 36, 42, 48) from each mesocosm and the Pacific. On the first sampling Day 0, samples were collected from the depth intervals 5–0 m and 17–5 m. From Day 8 onwards, sampling depths were 10–0 m and 17–10 m. Until Day 20, samples were regularly taken from both sampling depth intervals, after Day 20 only the upper interval (10–0 m) was sampled for microzooplankton, because concentrations in the deeper layer were too low to reach detection limits.

2.3 Abundance and species determinations

In the laboratory, the net samples taken for abundance/biomass determination of each mesocosm were split in half (Motoda splitter) and one half of each sample was preserved in 4 % formaldehyde-seawater solution for subsequent microscopic species identification and enumeration. The other half was used for ZooScan analyses. The formalin-preserved abundance subsample was split applying the Hunstman Marine Laboratory (HML) beaker technique producing count results with a coefficient of variation of 9–15 % from the effective mean (van Guelpen et al., 1982). Subsequently, aliquots were counted under a stereomicroscope (Nikon SMZ 1270) until at least 50 individuals of the most abundant taxa were counted, rare species/taxa were counted from the whole sample. As usual, zooplankton abundances were calculated assuming 100 % filtering efficiency of the net. However, variation among samples is normally high, due to plankton patchiness and moreover variation is species-/taxon-specific (Wiebe and Holland, 1968).

2.4 ZooScan

For the scanning procedure, samples were split further (Motoda splitter) to ratios between 1:4 and 1:32 to avoid crowding in the scanning chamber. In the laboratory, samples were scanned on an Epson Perfection V750 Pro scanner in a modification of the ZooScan method (Gorsky et al., 2010) and a scan chamber constructed of a 21 cm by 29.7 cm (DIN A4) size glass plate with a plastic frame. Scans were 8 bit greyscale, 2400 dpi images (tagged image file format; *.tif). The scan area was partitioned into two halves (i.e. two images per scanned frame) to reduce the size of the individual images and facilitate the processing by ZooProcess/ImageJ. "Vignettes" and image characteristics of all objects were extracted with ZooProcess (Gorsky et al., 2010) and sorted sequentially by first clustering and naming using MorphoCluster (Schröder et al., 2020) and then predicting the remaining unsorted images using deep-learning features in Ecotaxa (http://ecotaxa.obs-vlfr.fr/, Picheral et al. (2017)). Automated image sorting was manually validated by experts. Individual biomass was derived from the image area of each object using published taxon-specific relationships (Lehette and Hernández-León, 2009).

2.5 Zooplankton grazing, gut fluorescence

Grazing rates of the dominant copepods *Paracalanus* sp. were analyzed with the gut fluorescence (GF) method (Mackas and Bohrer, 1976) via experimental determination of gut clearance rates (clearance coefficient). Clearance rate determination assumes that maximum gut fullness of organisms equals initial gut pigment in the gut clearance experiment (time point zero minutes, $T_{0\,min}$). The experimental identification of a clearance coefficient is accomplished through fluorescence determination of organisms' guts allowed for clearance over a series of time steps for a total period of ca. 1 h. At least eight time steps along the time axis are recommended. Hence, pre-determination of in situ daily maximum gut fullness is required, if maximum ingestion rates are to be estimated (Båmstedt et al., 2000).

Copepods often have diel feeding rhythms (Mackas and Bohrer, 1976). Therefore, prior to clearance rate determination of mesocosm copepods, the feeding rhythmicity and time of maximum gut fullness of dominant copepods (*Paracalanus* sp.) were examined twice over a 24 h cycle, both of copepods collected in the adjacent Pacific as well as of copepods collected in the mesocosms. Each time zooplankton net samples were taken, adult female copepods (the dominant copepodite stage) were picked and GF measured (see below for more details on the procedure). These investigations proved that copepods' feeding activities, i.e. times of maximum gut fullness, were highest at night between approx. 22:55 and 03:40 (Fig. 2). Therefore, sampling of zooplankton in the mesocosms for clearance rate determinations was done at night on occasions, during the night of Day 21/22 and during the night of Day 34/35. MeZP samples were collected in all mesocosms with the same Apstein net of 17 cm opening diameter as mentioned above but equipped with a $200\,\mu$m net bag and a non-filtering cod-end to collect organisms gently and prevent stress evacuation of their guts before retrieval of the net.

Determination of gut clearance rates and coefficients followed recommendations by Båmstedt et al. (2000). Immediately after retrieval of each net haul, the zooplankton sample was split in eight subsamples. One of the subsamples was immediately concentrated over a $200\,\mu$m mesh, the mesh carefully folded not to squash organisms, wrapped in aluminium foil, and immediately shock-frozen in liquid nitrogen to preserve the in situ-state of gut content upon catch (time-point 0 min, $T_{0\,min}$). The other seven subsamples ($T_{8\,min}$–$T_{56\,min}$) were each incubated in 500 ml filtered seawater ($20\,\mu$m) to allow copepods to evacuate their guts. After each eight minutes, one of the incubated subsamples was terminated (i.e. last sample after 56 min, $T_{56\,min}$) by concentrating the zooplankton on a $200\,\mu$m mesh, the mesh wrapped in aluminium foil and immediately shock-frozen in liquid nitrogen. The shock-frozen subsamples ($T_{0\,min}$–$T_{56\,min}$) were stored at –80° C until further processing in the home laboratories in Kiel.

Paracalanus (mostly *Paracalanus parvus*) was the dominant copepod taxon in all mesocosms and therefore was chosen for determination of gut clearance rate. In Kiel, depending on availability, between 8 and 52 individual adult female *Paracalanus* sp. were picked on crushed ice under a stereomicroscope (Wild Heerbrugg M3) from each of the frozen subsamples ($T_{0\,min}$–$T_{56\,min}$) into 2 ml cryovials placed in a labtop vial cooler at –15° C. This procedure was done at dimmed room light usually within half an hour to prevent destruction of fluorescent pigments (Båmstedt et al., 2000). Loaded vials were stored at –80° C until completion of all samples from all mesocosms. Subsequently, gut pigments were extracted in 1.2 ml 90 % acetone with the help of glass beads (0.5 mm diameter) in a Precellys Evolution HP Homogenizer at 10,000 RPM (9168 g) for 15 sec. Constant
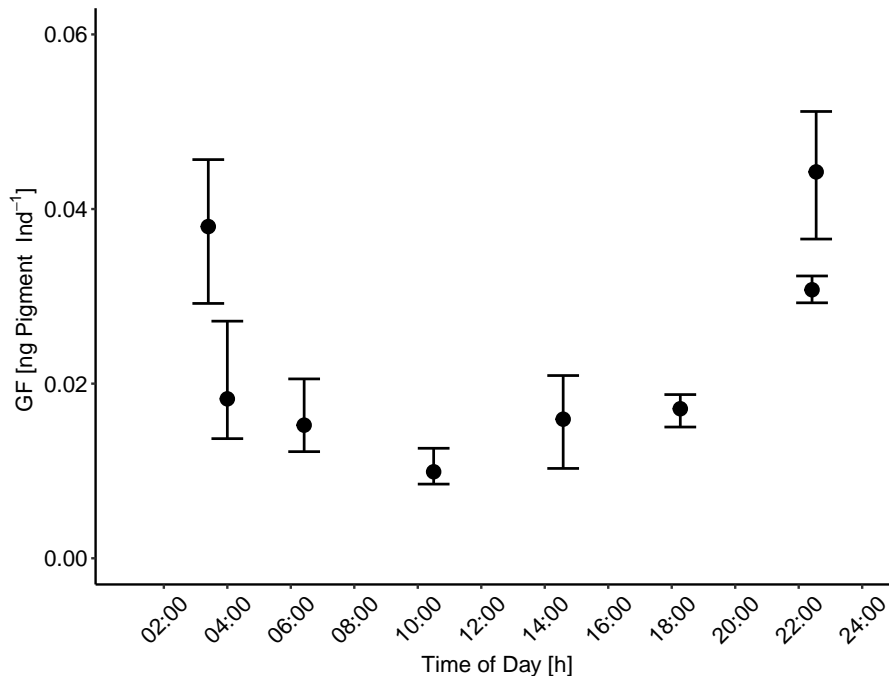
Figure 2. Gut fluorescence [ng Pigment Ind^{-1}]: diel feeding rhythm to determine time of maximum gut fullness of adult female *Paracalanus* sp.. Gut fluorescence was analyzed on females collected over a 24 h cycle in the mesocosms. Maximum gut fullness was detected early in the morning (03:44) and one hour before midnight (22:55). Error bars depict 95% confidence intervals.

cooling of samples was assured during the whole procedure to avoid pigment degradation. After 30 sec of pause, the crushed samples were treated in a Sigma 3–18K centrifuge for 10 min at 10,000 RPM (9168 g) at 4° C to separate liquid and solid
200 phase. Finally, the liquid phase was filtered through 0.2 μm PTFE filters to remove any remaining solid body parts. GF was then measured with a Trilogy Laboratory Fluorometer (Turner Design, USA). The relative GF of each sample was measured three consecutive times and converted to absolute values (ng pigment μg DM^{-1}) by means of a chlorophyll standard curve. To eliminate background fluorescence caused by astaxanthin carotenoids in copepod tissues, GF was corrected by GF measured of female *Paracalanus* collected in the surrounding Pacific and starved for 24 h to allow animals to empty their guts completely
205 (Mackas and Bohrer, 1976). An exemplary sample was analyzed for gut pigments (or their degradation products) also by means of reverse phase high performance liquid chromatography (HPLC, Barlow et al. (1997)) calibrated with commercial standards.

   To normalize GF, dry mass (DM) of female *Paracalanus* individuals was determined for each time-point subsample. Single female copepods were picked for DM determination of each sample in triplicate (i.e. three samples with one female from each mesocom, if enough organisms were available). Organisms picked for DM determination were rinsed in MilliQ, transferred into
210 pre-weighed tin cups before drying at 60° C for 24 h and mass determinations on a Mettler Toledo XP2U Ultra Micro Balance (accuracy: 0.000058–0.0034 μg). Additionally, females from Day 21/22 samples were picked for C:N determinations usually

from $T_{0\,min}$ and $T_{56\,min}$ (13–38 individuals per sample depending on availability). Carbon and nitrogen elemental analyses were done on a Euro EA – CHNSO Element Analyzer according to Sharp (1974).

2.6 Fatty acid analysis of dominant copepods

215 Adult females (the dominant developmental stage) of the dominant copepods *Paracalanus* sp. and *Hemicyclops* sp. were picked as soon as possible after collection for lipid analysis from the second net (for live organisms). Due to time constraints, female copepods were only picked from six mesocosms (M2, M3, M6 of the moderate treatment, M1, M4, M5 of the extreme treatment). Lipid samples of female copepods from the adjacent Pacific could only be picked during phase 3 because of limited abundance during phases 1 and 2. If available, up to 80 individuals (minimal 16) of each species were sorted to assure

220 sufficient lipid mass above detection limit. Some samples were directly transferred to dichloromethane:methanol (2:1, v/v) in 8 ml analytical vials equipped with teflon-sealed screw caps, and some were transferred to Eppendorf caps without solvent. The latter allowed for determination of DM after lyophilization. DM of specimens directly stored in dichloromethane:methanol (2:1, v/v) could not be determined. Samples were stored at –80° C until further analysis in the home laboratory at Bremen University.

225 DM of the copepods was determined after lyophilization for 48 h (CHRIST Alpha). Total lipids were extracted from the samples after Folch et al. (1957) and Hagen (2000) with dichloromethane:methanol (2:1 v/v). For quantification of total fatty acids (TFA), tricosanoic acid (23:0) was added as an internal standard prior to extraction and TFAs were expressed as the percentage of fatty acids in relation to the DM of the sample (TFA % DM). For *Paracalanus*, TFAs were related to mesocosm-specific mean DM of females used for gut fluorescence determination, because DM determined after lyophilization of lipid

230 samples was inaccurate. Lipid extraction of samples stored in solvent followed the same procedure as for the lyophilized samples.

Fatty acids were converted to their methylester derivatives (FAME) by transesterification for 4 h at 80° C in hexane and methanol containing 3 % concentrated sulphuric acid (Kattner and Fricke, 1986). FAMEs were extracted with aqua bidest. and hexane and analyzed by gas chromatography (Agilent Technologies, GC model 7890A). The device was equipped with a

235 DB-FFAP column (30 m length, 0.25 mm inner diameter) and a programmable temperature vaporizer injector, operating with helium as carrier gas (Peters et al., 2007). Fatty acid and alcohol components were detected using a flame ionization detector (FID) and identified by their retention times in comparison to known fatty acid and alcohol standard compositions (FAMEs and free alcohols of the copepod *Calanus hyperboreus* and Supelco 37 Component FAME Mix). In some cases, the lipid mass was very low with a stronger impact of impurities, so that gas chromatography did not result in reliable data. Therefore, data

240 presented here are those that have at least 70 % purity of fatty acids relative to impurities. The fatty acid compositions were evaluated according to the fatty acid trophic marker (FATM) concept of Dalsgaard et al. (2003).

2.7 Elemental composition (C, N, O, P) and stable isotope (δ^{13}C, δ^{15}N) signatures of mesozooplankton

Bulk samples of copepods or polychaetes were used for the analysis of stable isotope signatures (δ^{13}C and δ^{15}N) and carbon (C), nitrogen (N) and particulate organic phosphorus (POP) content. Copepod samples mainly contained the taxa *Paracalanus*

sp. and *Hemicyclops* sp., whereas polychaetes were separated into the species *Paraprionospio* sp. and *Pelagobia longicirrata*. Copepods and polychaetes were pipetted through a 55 μm nylon mesh attached to a polypropylene tube of $\sim$2 cm length, so that the organisms remained on the mesh. Organisms were shortly rinsed with MilliQ water. Bulk samples were transferred to pre-weighed tin capsules (5x9 mm, Hekatech) and dried at 60° C for at least 24 h. After drying, tin capsules were closed at the top and stored in a 96 well plate covered with Parafilm. In the home laboratories, samples were dried again and weighed on a microbalance. Subsamples for phosphorus were taken, whenever enough biomass of the sample was available. Target sample masses were 1–4 mg for C:N and 1–10 mg for POP. Stable isotopes (^{13}C and ^{15}N), C and N contents were analyzed at the UC Davis Stable Isotope Facility using a PDZ Europa ANCA-GSL elemental analyzer interfaced to a PDZ Europa 20-20 isotope ratio mass spectrometer (Sercon Ltd., Cheshire, UK) with helium as carrier gas. Vienna Pee Dee Belemnite and atmospheric air were used as standards to determine the carbon and nitrogen ratio, respectively. Stable isotope ratios are reported with reference to a standard and expressed in parts per thousand (‰) according to the formula $\delta^{H}X = [(R_{SAMPLE} / R_{STANDARD})]$, where X is the respective element, H gives the heavy isotope mass of that element, and R is the ratio of the heavy to the light isotope.

POP was determined photometrically on a Hitachi U-2900 Spectrophotometer as orthophosphate after oxidative decomposition by adding a spatula tip Oxisolv® 5 ml Milli-Q and the sample in Pyrex tubes and autoclaving. After cooling to room temperature, a subsample (dilution 1:5 or 1:10) was measured according to Ehrhardt and Koeve (1999).

2.8 Elemental composition (C, N, P) of microzooplankton

Samples for X-ray microanalysis (XRMA) were prepared following Segura-Noguera et al. (2012). 500 mL water samples were taken from each mesocosm and the Pacific Ocean and were pre-filtered through a 200 μm nylon mesh to remove larger mesozooplankton. The 200 μm–filtered water samples were further concentrated via inverse filtration (vacuum pump, 15 μm nylon mesh) to a volume of approximately 2–4 ml. These 2–4 ml remaining water samples were pipetted through a 15 μm nylon mesh, so that the organisms remained on the mesh, where they were rinsed several times with ice-cooled Milli Q brought to pH of 8.3–8.5 with NaOH. The last $\sim$50 μl were pipetted to a slide (in several drops) and checked under a stereomicroscope for microzooplankton organisms. 5 μl were transferred to a TEM grid (coated with a formvar carbon film on Copper on 75 mesh, Agar Scientific) in triplicates and again shortly checked under the stereomicroscope to ensure that there was a sufficient number of organisms from the same species to be analyzed. TEM grids were air-dried for about 1 h and afterwards transferred to TEM grid storage boxes and stored in a desiccator container (Fisherbrand™ Circular Bottom Desi-Vac™ Container, Fisher Scientific) until arriving in the home laboratories in Germany. Samples were then kept in vacuum bags until final analysis.

XRMA analysis were done at the Joseph Banks Laboratories in Lincoln, UK. Single cells of microzooplankton (200–20 μm) were imaged and analyzed for C, N, O, and P elemental content in a FEI Inspect Scanning Electron Microscope (SEM), equipped with an energy-dispersive spectrometer Oxford X-Act silicon drift detector (SDD). X-ray spectra were acquired from an area that circumscribe the cell, at 20 kV of accelerating voltage, accumulation time of 120 sec (life time), spot size 6.0, and 10 mm working distance. Following the analysis of each cell, a blank spectrum (i.e. formvar only) close to the cell was acquired for 30 sec lifetime. Spectra from cells that drifted, changed shape or charged during analysis were discarded. An image before

and after the analysis was taken using the INCA Oxford EDS software and the area of analysis was calculated with a MATLAB routine. X-ray bremsstrahlung from each spectrum was removed using NIST DTSA-II Jupiter 2017-11-06 and the intensity of each peak was also calculated with a MATLAB routine. The standards used for quantification were latex beads of 3 and 5 μm for C and ADP for N, O and P. Latex beads of 3 μm were analyzed as internal standards several times during each analysis session to correct for drift and for changes in day-to-day beam intensity. A detailed description of the measuring approach is given in Segura-Noguera et al. (2016).

2.9 Data evaluation, statistical analysis

We applied repeated measures ANOVA (rmANOVA) to test for possible treatment effects. Response variables (listed in Table 1) were modeled as a function of deep-water treatment (two levels: 'moderate' and 'extreme') and experiment day with mesocosm as random factor to test for significant differences between the added deep waters with different OMZ signature. Normality and variance homogeneity of residuals was tested graphically. In case of significant results, if assumptions were not met, data were log 10 transformed and re-analyzed. Unfortunately, ~50 % of the fatty acid samples showed a substantial level of impurities due to the generally very low lipid content of the copepods and, therefore, were omitted from the data set, i.e. only samples with at least 70 % purity are included in the present study. This led to a restricted data set with unbalanced sampling design and unequal and low number of replicates that didn't allow for more comprehensive statistics (rmANOVA). Instead, we calculated mean percentages and their 95 % confidence interval (CI) of the dominant fatty acids per mesocosm treatment and experimental phase to allow for basic statistical inference. Comparing any two means, evidence of significance can be inferred if their CIs do not overlap (Field et al., 2012). Similarly, initial GF values of copepods of each mesocosm (with standard deviation, SD) are shown together with treatment means and their 95% CIs, because measured GF in the copepods' guts of both OMZ treatments was too low to allow for grazing rate estimations.

Pearson correlations between abundance of the dominant zooplankton taxa, the copepods *Paracalanus* sp. and *Hemicyclops* sp., and counts of dominant phyto- and microzooplankton groups (diatoms, phytoflagellates, coccolithophores, dinoflagellates, silicoflagellates, ciliates, all in cells L^{-1}) and with concentrations of extracted phytoplankton pigments (Chloro-, Dino-, Crypto-, Prymnesio-, and Pelagophyceae, diatoms, *Synechococcus*, all in μg L^{-1}) and with total chlorophyll a (μg L^{-1}) were performed to gain insight into food web relations.

All statistics were performed using R 4.2.2 (libraries emmeans, lme4, lmerTest, and HighstatLib.V6 (R Core Team, 2014).

3 Results

3.1 Zooplankton abundance and contribution of taxonomic groups

Average total abundance of MeZP was very similar at the start of the experiment and no significant differences developed between the two OMZ deep-water treatments over the course of the experiment (Table 1). However, the established treatment differences with respect to N:P signatures were significant but only small. Thus, any potential small-scale treatment differences

in MeZP abundance, if existent at all, would have most likely been hidden by methodical uncertainties associated with net sampling, patchy distribution, and counting bias (Algueró-Muñiz et al., 2017; Lischka et al., 2017).

Variability of the manual counts of total mesozooplankton abundance (Individuals per Liter, Ind L^{-1}) was high between mesocosms and sampling days. Average total mesozooplankton abundance varied between 6.3 Ind L^{-1} (CI 3.5) on Day 30 and 52.7 Ind L^{-1} (CI 14.0) on Day 42 in the moderate-treatment mesocosms, and between 7.2 Ind L^{-1} (CI 3.3) on Day 30 and 33.9 Ind L^{-1} (CI 30.1) on Day 42 in the mesocosms with the extreme treatment. Total abundance of mesozooplankton sampled in the adjacent Pacific station was in a similar range as numbers estimated in the mesocosm treatments (9.7–129.3 Ind L^{-1}) and peaked on Day 48 (Fig. 3). Individual mesocosms developed some more distinct abundance peaks at the beginning and towards the end of the study with maximum numbers of 112.3 Ind L^{-1} in M1 on Day 10, 127.9 Ind L^{-1} in M4 on Day 42, and 129.0 Ind L^{-1} in M3 on Day 48. Deep-water additions on Day 11 and Day 12 after removal of approx. 20 m^3 of water from each of the mesocosms, respectively (Bach et al., 2020), resulted in distinct deviation from average mesozooplankton abundance between Day 13 and Day 18 with temporarily higher numbers in the moderate mesocosms. This deviation was only short-term and not significant but due to some higher abundance in M7 (moderate treatment) causing the relatively large confidence intervals (Table 1, Fig. S1) and had equalized by Day 24 but was indicative of different mesozooplankton densities of the two injected deep-water masses.

In terms of abundance, copepods dominated the zooplankton communities at all times both in the mesocosms and the adjacent Pacific. Other taxa (in descending order of contribution: Polychaeta, Echinodermata, Euphausiacea, Mollusca, Hemichordata, Cnidaria, Chordata, Cirripedia, Rotifera) contributed only between 0.2 % and 18 %. Higher shares of other taxa were found only until Day 18, afterwards they were negligible. This pattern essentially reflected the occurrence of copepods and other taxa in the surrounding Pacific (0.3–24 %), although in the Pacific other taxa contributed higher shares to the zooplankton community compared to the values found in the mesocosms also after Day 18 (Fig. 4a).

Among other taxa, in the mesocosms, Polychaeta, Echinodermata, Euphausiacea, and Mollusca (taxa ordered in decreasing trend) were most abundant, sometimes constituting more than 5 % of total abundance. Remaining taxa consistently contributed less than 5 % to total mesozooplankton abundance. Towards the end of the study, the numbers of Chordata (ichthyoplankton) and Cnidaria increased in M1, M2, M4, M5, and M6 to values >1 %. In the Pacific in the early phase of the experiment, Polychaeta (up to 21 %) and Echinodermata (up to 11 %) dominated, followed by Hemichordata (2 %) and Rotifera (3 %). In the second half of the experiment, Polychaeta, Cirripedia, Mollusca, and Chordata (each <3 %) dominated the generally low share of other taxa on total abundance. Chordata (ichthyoplankton) increased because fish eggs were added to the mesocosms on Day 31, however they did not stay for long in the mesocosms (Bach et al., 2020) (Fig. 4b).

3.1.1 Dominant copepods

The enclosed copepod community was dominated by *Hemicyclops* sp. at time of mesocosm closure. *Hemicyclops* sp. continued to dominate in the moderate treatment almost throughout the experiment (up to 65% on Day 36), whereas in the mesocosms of the extreme treatment, after the deep water addition *Paracalanus* sp. increased to similar percent contributions as *Hemicyclops* (up to 54% on Day 18, and up to 60% on Day 13, respectively) (Fig. 5). The genus *Paracalanus* comprised two different

Table 1. Results of repeated measures ANOVAs. OMZ treatments (levels: moderate, extreme) and experiment day (Tday = Day 13 – Day 48) served as independent variables (FACTOR). Abundance and biomass of zooplankton categories and stable isotope content of copepods served as dependent variables and are listed below as RESPONSE. Mesocosm was used as random effect in the linear models. Response variables that were log 10 transformed are indicated (*log 10*). Alpha level for $p = 0.05$. Note: Single effects of experiment day (time) are not listed as they are not of interest in the present study, but were for most response variables significant ($p > 0.05$).

FACTOR	OMZ treatment			OMZ Treatment*Tday			Corresponding figure
	df	*F*	*p*	*df*	*F*	*p*	
RESPONSE							
ABUNDANCE [Ind L^{-1}]							
Mesozooplankton	1	0.5506	0.486	6	0.5562	0.765	Fig. 3
Acartia sp.	1	0.0120	0.916	5	1.5344	0.209	Fig. 5
Hemicyclops sp.	1	1.9189	0.173	6	1.3780	0.245	Fig. 5
Harpacticoida	1	0.5916	0.471	6	0.4214	0.860	Fig. 5
Nauplii	1	0.1826	0.684	6	1.1284	0.366	Fig. 5
Oithona sp.	1	1.3754	0.286	6	0.6983	0.653	Fig. 5
Oncaea	1	0.3168	0.594	6	0.6191	0.714	Fig. 5
Others	1	2.9816	0.126	6	0.6618	0.681	Fig. 5
Paracalanus sp.	1	1.0691	0.341	6	0.5958	0.732	Fig. 5
Acartia sp. adults	1	0.6375	0.456	6	1.1083	0.374	Fig. 6
Acartia sp. copepodis	1	1.3223	0.294	6	0.7522	0.612	Fig. 6
Hemicyclops sp. adults (*log 10*)	1	0.3897	0.534	6	0.5622	0.759	Fig. 6
Hemicyclops sp. copepodids	1	4.7703	0.071	6	1.1369	0.357	Fig. 6
Oncaea sp. adults	1	0.2205	0.654	6	0.7794	0.589	Fig. 6
Oncaea sp. copepodids	1	0.2510	0.634	1	1.0910	0.336	Fig. 6
Paracalanus sp. adults	1	0.7651	0.418	6	0.4991	0.807	Fig. 6
Paracalanus sp. copepodids	1	0.8243	0.399	6	1.3424	0.261	Fig. 6
BIOMASS [μg DM L^{-1}]							
Acartia sp.	1	0.4639	0.521	6	0.6052	0.724	Fig. 8
other Calanoida	1	0.6568	0.422	6	0.4126	0.866	Fig. 8
Copepoda (*log 10*)	1	1.9581	0.169	6	0.5117	0.796	Fig. 7
other Cyclopoida	1	1.1426	0.326	6	2.1171	0.075	Fig. 8
Hemicyclops sp. (*log 10*)	1	4.7292	0.073	6	0.3362	0.913	Fig. 8
Oncaea sp.	1	3.6411	0.063	6	1.8365	0.115	Fig. 8
Paracalanus sp.	1	1.6099	0.212	6	0.8348	0.550	Fig. 8
Polychaeta	1	0.4603	0.523	6	0.1567	0.986	Fig. 7
STABLE ISOTOPES							
δ^{13}C	2	4.2743	0.082	12	1.7068	0.117	Fig. 9
δ^{15}N	1	2.0349	0.203	6	0.2741	0.945	Fig. 9

species, *P. parvus* and *P.* cf. *quasimodo*. *P. parvus* was numerically dominant and occurred with all copepodite stages. *P.* cf. *quasimodo* was found only in the adult stage.

The variability of the percentage share over time of *Hemicyclops* sp. and *Paracalanus* sp. in the surrounding waters of the Pacific was higher than observed in the mesocosms.
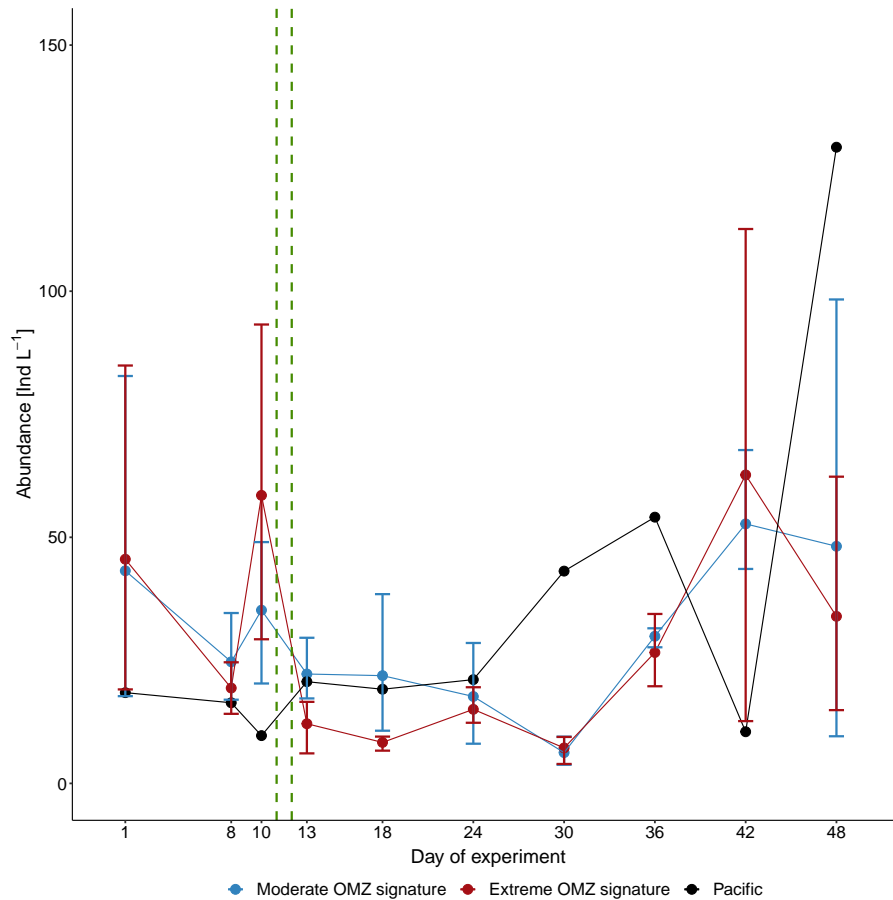
Figure 3. Average total abundance of mesozooplankton (Individuals per Liter, Ind L^{-1}) in the mesocosms with moderate and extreme OMZ signatures and the adjacent Pacific station. Error bars depict 95 % confidence intervals. The green vertical dashed lines indicate the days of OMZ water additions.

Acartia sp., usually the dominant neritic species in these coastal upwelling areas, was consistently low in both mesocosm treatments (up to 1 % mean portions), whereas it ranged between 0.1–30 % in the adjacent Pacific. Five different species of the
350   cyclopoid genus *Oncaea* were registered. *Oncaea venusta*, *O*. cf. *chiquito*, and three other *Oncaea* species that could not be identified to species level. Especially in the second half of the experiment, *Oncaea* sp. was the third most abundant copepod genus in both treatments. The cyclopoid genus *Oithona* occurred with four different species, *O. nana*, *O*. cf. *nana* and two undetermined *Oithona* species. *Oithona* sp. had consistently low abundances in the mesocosms (<1 %) but contributed 10.6 % on Day 30 in the adjacent Pacific.
355   Harpacticoid copepods occurred in the mesocosms in the beginning but decreased quickly after the start of the experiment in both treatments (≤8 %). The succession of harpacticoid copepods in the surrounding Pacific was more variable than in the mesocosms (8–33 %). Opposite to the adjacent Pacific, the occurrence of copepod nauplii in the mesocosms was low during
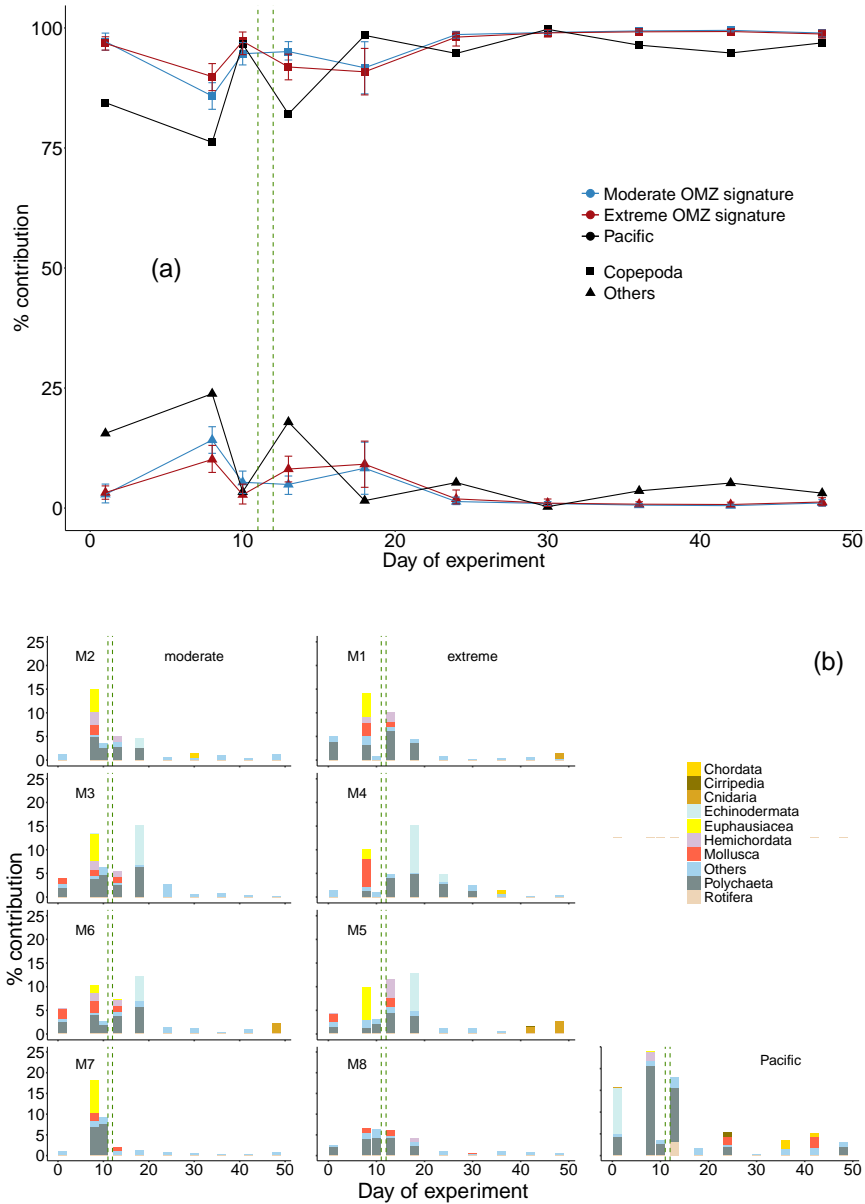
Figure 4. Percent contribution of major taxonomic groups on total mesozooplankton abundance. (a) Copepoda and "Others" (Chordata, Cirripedia, Cnidaria, Echinodermata, Euphausiacea, Hemichordata, Mollusca, Polychaeta, Rotifera). Shown is the mean across OMZ treatments (moderate and extreme signature mesocosms, respectively) with 95 % confidence intervals and the contribution of Copepods and "Others" in the Pacific. (b) percent contribution of "Others" shown in the upper panel split into taxonomic groups. Category "Others" summarizes all taxonomic groups that contributed less than 1 % on a particular sampling day. The green vertical dashed lines indicate the days of OMZ water additions.
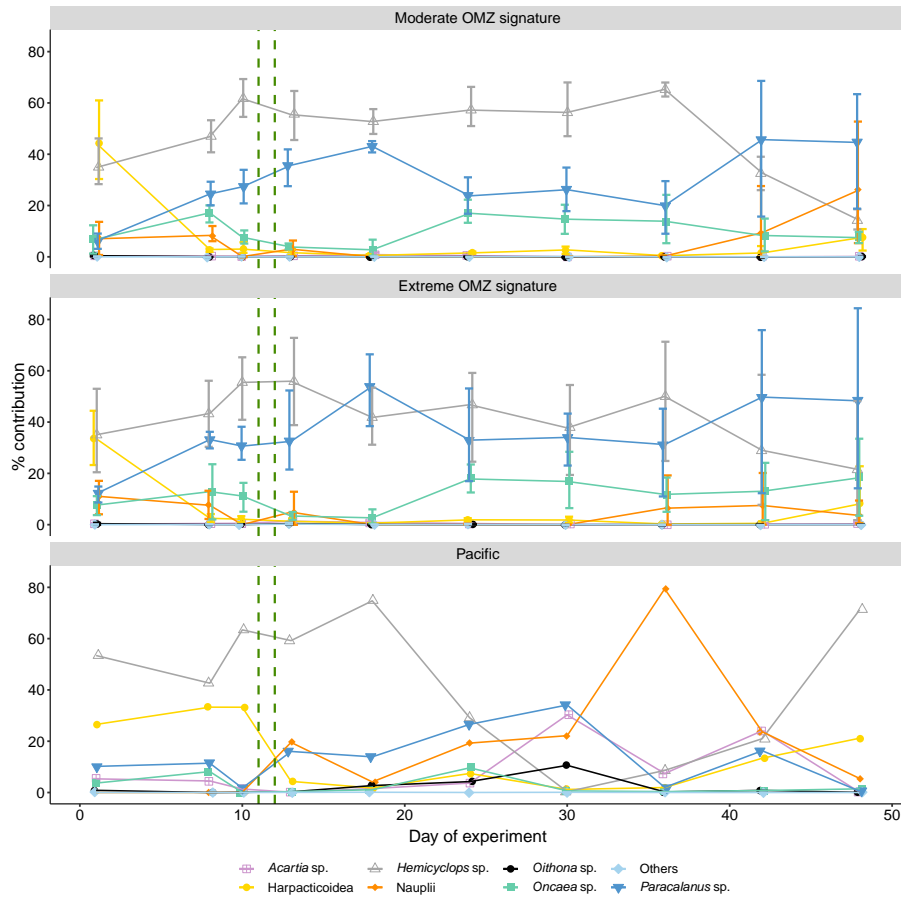
Figure 5. Percent contribution of copepod genera and copepod nauplii on total copepod abundance. Shown is the mean across OMZ treatments (moderate and extreme signature mesocosms, respectively) with 95 % confidence intervals and the contribution of each category in the Pacific. Category "Others" comprises copepods of the genera *Calanus*, *Centropages*, *Clausocalanus*, *Corycaeus*, *Clytemnestra*, *Eucalanus*, *Euterpina*, *Labidocera*, *Mecynocera*, *Microsetella*, *Scolecithrix*, *Temora*. The green vertical dashed lines indicate the days of OMZ water additions.

most of the experiment in both treatments. In the moderate treatment, nauplii contributed between 9.4 % and 0 % over time. Only towards the end of the experiment nauplii increased to 26.2 %. In the extreme-treatment mesocosms nauplii contribution varied between 14.8 % and 3.6 %. Nauplii contribution in the surrounding Pacific was almost consistently higher than in the mesocosms (up to 79 %).

Copepods of the category "Others" comprised the genera *Calanus*, *Centropages*, *Clausocalanus*, *Corycaeus*, *Clytemnestra*, *Eucalanus*, *Euterpina*, *Labidocera*, *Mecynocera*, *Microsetella*, *Scolecithrix*, and *Temora*. This category accounted on average for less than 1 % of total copepod abundance in all mesocosms as well as the Pacific during the whole experiment duration.
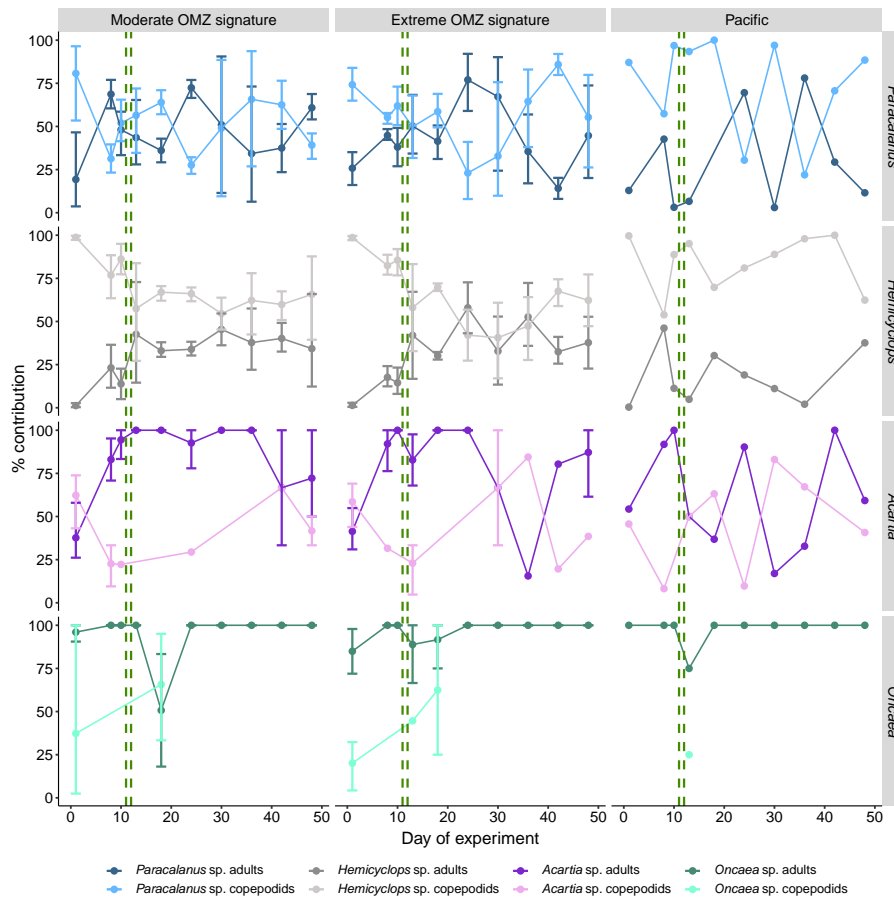
Figure 6. Temporal succession of developmental stages of dominant copepods (average % contribution on total genus abundance with 95 % confidence intervals). Adults comprise of female and male copepods, copepodids comprise of stages CI–CV. The green vertical dashed lines indicate the days of OMZ water additions.

365   For none of these species or groups significant effects between the mesocosm deep-water treatments were determined (Table 1).

3.1.2   Succession of developmental stages of dominant copepods

Overall, succession patterns of developmental stages of the different copepod species in the mesocosms did not vary significantly between the deep-water treatments. In case of *Paracalanus* sp. and *Hemicyclops* sp. copepodids usually outnumbered

370   adults in both mesocosm treatments (Fig. 6), only sporadically, adults accounted for more than 60–70 %. The stage contribution of *Paracalanus* in the Pacific was mostly in favour of copepodids (usually >50 %), except for Day 24 and Day 36 with >70 % adult copepods. The portion of *Hemicyclops* copepodids in the surrounding Pacific was consistently higher throughout the experiment and always higher than 50 %. *Acartia* sp. copepodids dominated in both mesocosm treatments at experiment start.

Thereafter, the population matured and consisted predominantly of adult copepods. The stage distribution of *Acartia* sp. in the surrounding Pacific was more variable. *Oncaea* sp. almost exclusively occurred in the adult stage, both in the mesocosms and the Pacific.

3.2 Zooplankton biomass

For the dominant taxa, the Zooscan method reduced the systematic variability, and added the size information for each object, allowing biomass estimation. For rare taxa, manual enumeration is to be preferred because of the low split ratios in the scans.

Zooplankton biomass (as estimated based upon scanned area of individuals) was dominated by copepods (Fig. 7a), which in the mesocosms ranged between 11.8 and 75.6 μg DM L^{-1} in the first phase, increased to between 8.58 and 137.9 μg DM L^{-1} in the second phase and declined again to between 4.8 and 40.8 μg DM L^{-1} in the third phase. The second most important contributor to zooplankton biomass were polychaetes (Fig. 7b), which in the mesocosms were hardly detected at Day 1 and ranged between 0 and 39.0 μg DM L^{-1} in the first phase, between 0 and 74.7 μg DM L^{-1} in the second phase, and between 0 and 0.65 μg DM L^{-1} in the third phase, respectively. Highest biomass values were observed for both total copepods and polychaetes in mesocosms M2 and M3 (both in the moderate mesocosm treatment). The main contributors to copepod biomass were *Paracalanus* sp. and *Hemicyclops* sp.. Due to the high variability between mesocosms, however, this treatment effect was insignificant (Table 1). In the adjacent Pacific, total copepod and polychaete biomass tended to be lower than in the experimental mesocosms but followed a similar temporal pattern (peaking in phase 2). Among the copepods, the numerically dominant genera *Paracalanus* and *Hemicyclops* were also the main biomass contributors (Fig. 8a and b), with roughly equal share and peaking in phase 2, in particular in the moderate OMZ signature treatments. *Acartia*, which was only present in lower abundance/biomass (Fig. 8c), tended to reach higher biomass in the extreme OMZ signature treatments (in particular in M4). *Oncaea* and other/unidentified cyclopoids (Fig. 8d, f) were mainly present in the first phase 1, with lowest values in phase 2 and a slight increase in phase 3.

In contrast to MeZP abundance, biomass (copepods) peaked between Day 10 and Day 20, but highest abundance values were found towards the end of the experiment when biomass was at a minimum. This discrepancy is most likely due to a shift in the abundance/biomass relationship of dominating zooplankton organisms towards smaller size or lower mass individuals, respectively.

3.3 Zooplankton grazing, gut fluorescence

In general, initial (T$_{0 \text{ min}}$) GF of *Paracalanus* sp. females was very low, but averages for the moderate and the extreme treatment, respectively, on Day 34/35 (0.14 and 0.29 ng pigment μg DM^{-1}) were higher than on Day 21/22 (0.03 and 0.08 ng pigment μg DM^{-1}), indicating somewhat higher feeding activities of *Paracalanus* females on autotrophic food particles later in the experiment (Table 2). Due to such low GF, no clearance rate measurements could be inferred, because GF of incubated copepods showed no clear decreasing trend in GF over time (data published at PANGAEA, https://doi.org/10.1594/PANGAEA.947833, Lischka et al. (2022).) Female *Paracalanus* of the adjacent Pacific had even lower fluorescence in their guts (0.005 and -0.004 ng pigment μg DM^{-1}) than measured in mesocosm organisms.
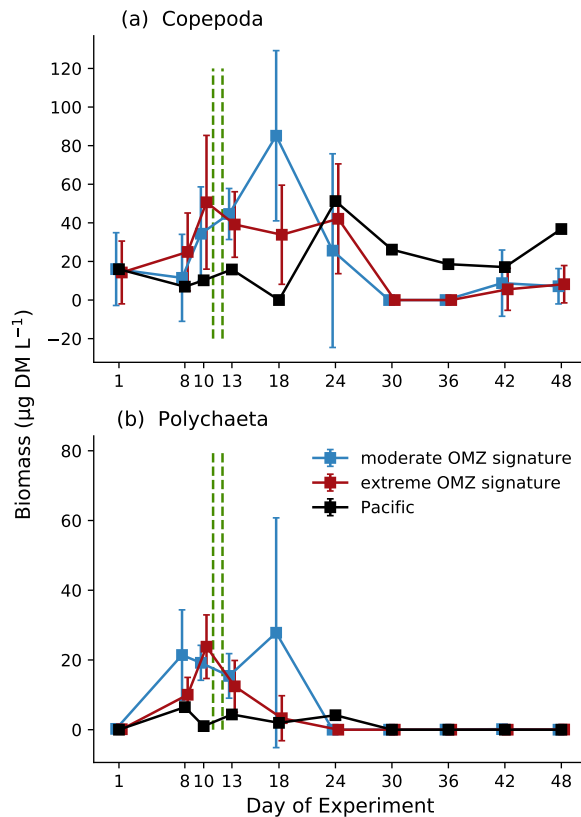
Figure 7. Biomass development (μg DM L^{-1}) averaged for the moderate and extreme treatments over time of total copepods (a) and poly-chaetes (b) based on image analysis (Zooscan). Blue = moderate OMZ signature, red = extreme OMZ signature, black = Pacific. Error bars depict 95 % confidence intervals. The green vertical dashed lines indicate the days of OMZ water additions. The experimental phase 1 lasted from Day 1 until Day 11/12, phase 2 until Day 40, phase 3 until experiment termination. Note different y-axis scale.

An attempt to analyze gut fluorescence with HPLC to identify degradation products (phaeopigments) of chlorophyll a and conclude on potential food sources (Welschmeyer, 1994) revealed no identifiable peak(s) besides astaxanthin indicative of the copepods' carapax, supporting very low GF, thus very low feeding on autotrophic food particles.

410   Mean C:N values for copepods in mesocosms treated with St. 3 (extreme) and St. 1 (moderate) OMZ water, respectively, were 5.40 and 4.99 and had overlapping CIs, thus no significant differences are suggested. Availability of female *Paracalanus* during Day 34/35 was not sufficient to reach the detection limit for C:N analysis.

3.4 Lipids

Fatty acid (FA) analyses revealed a relatively high degree of impurities of the samples. This is a common problem in small
415   copepods with rather low total lipid mass close to the detection limit (Lischka and Hagen, 2007). For this reason, identification
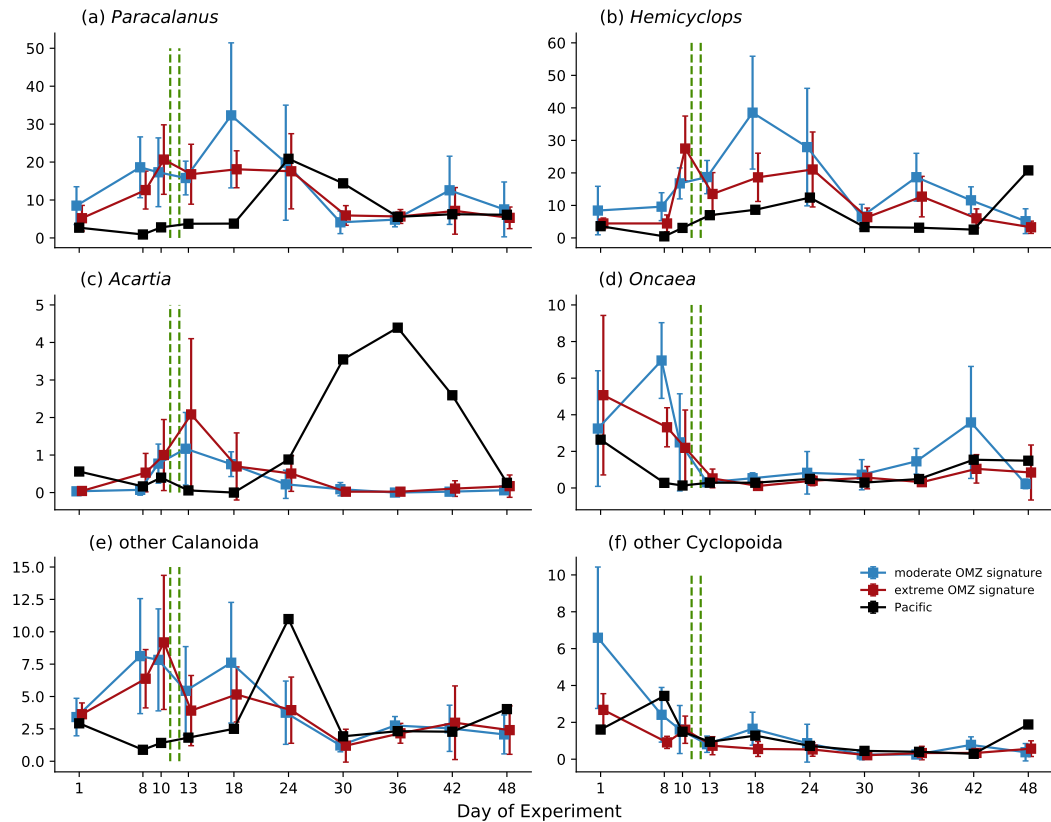
Figure 8. Biomass (μg DM L^{-1}) development averaged for the moderate and extreme treatments of major taxonomic groups during the course of the experiment. Error bars depict 95 % confidence intervals. The green vertical dashed lines indicate the days of OMZ water additions. The experimental phase 1 lasted from Day 1 until Day 11/12, phase 2 until Day 40, phase 3 until experiment termination. Note different y-axis scale.

of FA peaks in the gas chromatogram was sometimes difficult or even impossible. Therefore, data presented here only include results of samples of which at least 70 % of all peaks of a chromatogram could be identified and assigned to a specific FA (i.e. 70 % purity).

3.4.1 Total fatty acids

420   Total fatty acid content (TFA in % DM, equivalent to total lipid levels) of *Paracalanus* sp. (females) from the mesocosms were low (1.5–4.2 % DM) throughout the study period and did not vary significantly between the phases and treatments as indicated by overlapping CIs (Table 3). Mean TFAs of individuals collected in the adjacent Pacific during phase 2 fall within the range of TFA levels determined for the mesocosm copepods. Only one copepod sample from the Pacific could be analyzed in phase 3 where TFAs contributed 0.5 % to DM.

Table 2. Gut fluorescence (GF, ng pigment μg DM^{-1}) of *Paracalanus* females collected during the night of 18/19 March 2017 (Day 21/22) and during the night of 31 March/01 April 2017 (Day 34/35) immediately frozen after net retrieval onboard to preserve in situ GF (initial gut fluorescence, i.e. $T_{0\,min}$). Standard deviation (SD), 95 % confidence intervals (CI), C:N values are only available for Day 21/22 and are given as mol/mol.

	GF (ng pigment μg DM^{-1})		
	Day 21/22		Day 34/35
Mesocosm	Initial	C:N	Initial
OMZ signature of station 3 (moderate)			
2	0.008	5.51 (SD 1.00)	0.207
3	0.090	6.31 (SD 0.05)	0.196
6	–	4.57 (–)	0.099
7	0.018	4.98 (SD 0)	0.052
Mean	0.034 (0.038)	5.40 (CI 0.58)	0.139 (CI 0.074)
OMZ signature of station 1 (extreme)			
1	0.012	4.92 (SD 0.14)	0.014
4	0.089	5.74 (SD 0.12)	0.853
5	0.029	4.57 (SD 0.02)	0.148
8	0.171	4.76 (SD 0.15)	0.156
Mean	0.075 (0.072)	4.99 (CI 0.48)	0.293 (CI 0.371)
Pacific	0.005	5.68 (0.31)	-0.004

During phase 1, *Hemicyclops* sp. was not numerous enough for TFA determination, but sufficient numbers of organisms were available for lipid analyses during phase 2 and 3. In these two phases, TFA levels of *Hemicyclops* sp. in both treatments ranged between 5.3 % DM and 9.3 % DM. During phase 3 in the moderate treatment, mean TFA levels were comparatively high (9.3 % DM), but CIs suggest no significant differences between treatments and phases. The TFA level of female *Hemicyclops* sp. collected in the Pacific was comparable with the mesocoms treatments during both phases.

3.4.2 Fatty acid and fatty alcohol composition

The fatty acid (FA) and fatty alcohol (FAlc) composition is presented as mean contribution per experimental phase and OMZ treatment of specific FAs and FAlcs to total FAs and FAlcs of *Paracalanus* and *Hemicyclops* together with their CIs (Table 3). Only FAs that reached mean contributions of 2 % during at least one of the three phases and the sum of FAlcs were included in

Table 3. Fatty acid compositions (% TFA) of females of *Paracalanus* sp. and *Hemicyclops* sp. (mean contributions (%) and confidence limits (CI)) per treatment and phase of dominant fatty acids as well as the percentage of saturated (SFA), polyunsaturated (PUFA) fatty acids and free fatty alcohols (FAlc). Presented are only data of samples, where the contribution of FAs in relation to impurities was at least 70 %. Of those, only FAs are listed, where the phase mean was $\geqslant 2$ % at least during one occassion. Note: For *Paracalanus* TFA were related to mesocosm-specific average dry mass (DM) of weighed females collected for gut fluorescence; in case of *Hemicyclops* DM could be determined after lyophylization of copepod samples for lipid analysis and was subsequently used for calculation of % TFA. Phase 1: Day 1 to OMZ water addition (Day 11/12), phase 2: starting with the OMZ water addition until Day 40, phase 3: Day 40 until experiment termination.

		Paracalanus sp.				*Hemicyclops* sp.			
Treatment		extreme	moderate	adjacent Pacific		extreme	moderate	adjacent Pacific	
	FA	(M1, M4, M5)	(M2, M3, M6, M7)	(field samples)	n (St. 3, St. 1, Pacific)	(M1, M4, M5)	(M2, M3, M6, M7)	(field samples)	n (St. 3, St. 1, Pacific)
Phase									
1	TFA (% DM)	4.2 ($\pm$1.5)	3.8 ($\pm$0.7)	–	(n = 6, 5, 0)	–	–	–	(n = 0, 0, 0)
2		2.9 ($\pm$1.5)	2.3 ($\pm$0.7)	1.6 ($\pm$1.0)	(n = 13, 4, 2)	5.9 ($\pm$0.8)	5.9 ($\pm$8.0)	4.7 (–)	(n = 6, 6, 1)
3		1.5 ($\pm$1.5)	1.7 ($\pm$0.9)	0.5 (–)	(n = 6, 2, 0)	5.3 ($\pm$2.0)	9.3 ($\pm$4.0)	7.7 ($\pm$8.0)	(n = 6, 6, 2)
1	14:0	4.7 ($\pm$1.1)	4.7 ($\pm$1.0)	–	(n = 4, 4, 0)	–	–	–	(n = 0, 0, 0)
2		3.1 ($\pm$0.6)	2.8 ($\pm$0.5)	–	(n = 6, 8, 0)	2.1 ($\pm$0.1)	2.0 ($\pm$0.6)	–	(n = 6, 2, 0)
3		–	2.4 ($\pm$0.8)	5.5 (–)	(n = 4, 0, 0)	3.0 ($\pm$0.9)	3.1 ($\pm$0.9)	1.9 ($\pm$0.6)	(n = 3, 4, 2)
1	16:0	17.6 ($\pm$1.8)	19.1 ($\pm$2.9)	–	(n = 4, 4, 0)	–	–	–	(n = 0, 0, 0)
2		22.5 ($\pm$3.2)	20.9 ($\pm$3.4)	–	(n = 6, 8, 0)	21.7 ($\pm$1.6)	20.3 ($\pm$0.8)	–	(n = 6, 2, 0)
3		–	19.7 ($\pm$2.4)	23.9 (–)	(n = 4, 0, 0)	24.3 ($\pm$5.3)	24.1 ($\pm$0.7)	16.7 ($\pm$5.0)	(n = 3, 4, 2)
1	16:1(n-7)	**5.2 ($\pm$2.7)**	**5.0 ($\pm$2.9)**	–	(n = 4, 4, 0)	–	–	–	(n = 0, 0, 0)
2		1.2 ($\pm$0.3)	1.3 ($\pm$0.3)	–	(n = 6, 8, 0)	2.9 ($\pm$1.2)	2.7 ($\pm$0.6)	–	(n = 6, 2, 0)
3		–	2.0 ($\pm$1.0)	10.1 (–)	(n = 4, 0, 0)	2.3 ($\pm$0.8)	3.1 ($\pm$0.5)	2.9 ($\pm$1.9)	(n = 3, 4, 2)
1	18:0	7.0 ($\pm$1.9)	7.9 ($\pm$2.6)	–	(n = 4, 4, 0)	–	–	–	(n = 0, 0, 0)
2		14.7 ($\pm$5.3)	13.6 ($\pm$8.0)	–	(n = 6, 8, 0)	9.5 ($\pm$2.3)	9.7 ($\pm$1.1)	–	(n = 6, 2, 0)
3		–	9.4 ($\pm$0.7)	9.2 (–)	(n = 4, 0, 0)	16.1 ($\pm$9.8)	8.0 ($\pm$1.9)	10.1 ($\pm$2.4)	(n = 3, 4, 2)
1	20:5(n-3)	21.7 ($\pm$5.9)	20.7 ($\pm$5.7)	–	(n = 4, 4, 0)	–	–	–	(n = 0, 0, 0)
2		12.2 ($\pm$2.6)	12.4 ($\pm$2.6)	–	(n = 6, 8, 0)	7.9 ($\pm$0.6)	8.4 ($\pm$0.9)	–	(n = 6, 2, 0)
3		–	16.3 ($\pm$2.9)	21.0 (–)	(n = 4, 0, 0)	10.3 ($\pm$6.6)	8.5 ($\pm$0.7)	29.7 ($\pm$34.2)	(n = 3, 4, 2)
1	22:5(n-3)	1.4 ($\pm$0.3)	0.7 ($\pm$0.8)	–	(n = 4, 4, 0)	–	–	–	(n = 0, 0, 0)
2		1.0 ($\pm$0.5)	0.0 ($\pm$0.0)	–	(n = 6, 8, 0)	1.5 ($\pm$0.1)	2.0 ($\pm$0.5)	–	(n = 6, 2, 0)
3		–	0.0 ($\pm$0.0)	2.4 (–)	(n = 4, 0, 0)	1.1 ($\pm$0.8)	0.9 ($\pm$0.9)	1.8 ($\pm$1.2)	(n = 3, 4, 2)
1	22:6(n-3)/24:1(n-7)	33.4 ($\pm$9.1)	34.3 ($\pm$4.8)	–	(n = 4, 4, 0)	–	–	–	(n = 0, 0, 0)
2		34.8 ($\pm$7.7)	38.5 ($\pm$8.2)	–	(n = 6, 8, 0)	47.4 ($\pm$5.0)	46.7 ($\pm$3.3)	–	(n = 6, 2, 0)
3		–	45.8 ($\pm$2.4)	20.9 (–)	(n = 4, 0, 0)	35.0 ($\pm$10.5)	46.7 ($\pm$2.8)	27.3 ($\pm$17.0)	(n = 3, 4, 2)
1	SFA	31.8 ($\pm$3.1)	34.2 ($\pm$6.0)	–	(n = 4, 4, 0)	–	–	–	(n = 0, 0, 0)
2		43.7 ($\pm$8.8)	40.3 ($\pm$11.6)	–	(n = 6, 8, 0)	36.3 ($\pm$4.5)	35.2 ($\pm$1.9)	–	(n = 6, 2, 0)
3		–	33.7 ($\pm$3.5)	39.8 (–)	(n = 4, 0, 0)	47.2 ($\pm$14.2)	37.8 ($\pm$1.8)	31.5 ($\pm$10.5)	(n = 3, 4, 2)
1	PUFA	59.8 ($\pm$2.3)	58.5 ($\pm$7.9)	–	(n = 4, 4, 0)	–	–	–	(n = 0, 0, 0)
2		50.1 ($\pm$10.1)	54.0 ($\pm$11.3)	–	(n = 6, 8, 0)	58.2 ($\pm$5.2)	58.6 ($\pm$3.3)	–	(n = 6, 2, 0)
3		–	62.4 ($\pm$2.8)	48.4 (–)	(n = 4, 0, 0)	47.4 ($\pm$13.8)	56.5 ($\pm$2.3)	62.0 ($\pm$14.6)	(n = 3, 4, 2)
1	FAlc	0.7 ($\pm$0.7)	0.6 ($\pm$1.1)	–	(n = 4, 4, 0)	–	–	–	(n = 0, 0, 0)
2		1.9 ($\pm$1.6)	1.0 ($\pm$0.6)	–	(n = 6, 8, 0)	0.6 ($\pm$0.6)	1.3 ($\pm$1.2)	–	(n = 6, 2, 0)
3		–	0.5 ($\pm$0.1)	0 (–)	(n = 4, 0, 0)	0.9 ($\pm$0.4)	0.8 ($\pm$1.0)	1.4 ($\pm$0.2)	(n = 3, 4, 2)

the list. Generally, mean FA and FAlc compositions of both species did not differ much over time and treatment as suggested by overlapping CIs.

435

Dominant FAs in *Paracalanus* females were 20:5(n-3) and 22:6(n-3)/24:1(n-7), typical biomembrane components. Unfortunately, the peaks of the FAs 22:6 and 24:1 overlapped in the gas chromatogram and could not be separated in all cases, although a dominance of the ubiquitous 22:6(n-3) can be assumed. The mean percentage of 20:5(n-3) varied between 12 % and 22 % TFA between phases and treatments, and was similar in the Pacific females (21% during phase 3. The percentage of the 22:6(n-3)/(24:1(n-7) FA was higher in mesocosm females (33–46 % TFA) than in females from the Pacific (21 % TFA) 16:0, another important biomembrane component, occurred in higher concentrations (18–24 %) during all phases, both in females from the mesocosm and the Pacific. Biomarker FAs such as 16:1(n-7) and 18:1(n-7) typical of diatoms were consistently low. 16:1(n-7) ranged between 1 % and 5 % TFA in mesocosm females, with CIs indicating some higher contribution during phase 1 compared to phases 2 and 3 in both treatments which could be indicative of diatom feeding during phase 1 when this phytoplankton group dominated (Bach et al., 2020). In *Paracalanus* females sampled in the adjacent Pacific during phase 3, 16:1(n-7) contributed 10% to TFA. The percentage of 18:1(n-7) was consistently below 1 % and is therefore not listed in Table 2. Mean phase contributions of all other FAs were usually below 10 % TFA, except for 18:0 with up to 15 % during phase 2.

The FA signature of *Hemicyclops* females was similar to that of *Paracalanus*. The biomembrane FAs 16:0, 20:5(n-3), and 22:6(m-3)/(24:1(n-7) dominated. The portion of 16:0 varied between 20 % and 24 % TFA in mesocosm females and was somewhat higher than in females collected in the Pacific (17%). The mean contributions of 20:5(n-3) ranged between 8 % and 10 % TFA in mesocosm females, while in females from the Pacific this FA comprised 30 % TFA. 22:6(n-3)/(24:7(n-7) ranged from 35 % to 48 % TFA in mesocosm females and contributed 28 % TFA in females collected in the Pacific. The share of the diatom biomarker FAs 16:1(n-7) and 18:1(n-7) was very low, between 2 % and 3 % TFA in case of 16:1(n-7) and below 2 % TFA for the latter (and therefore not listed in Table 3). Of the remaining FAs, only 18:0 reached contributions between 9 % and 16 %, all others were below 3 % TFA.

PUFAs, mainly 20:5(n-3) and 22:6(n-3)/24:1(n-7), of female *Hemicyclops* and *Paracalanus* ranged between 50 % and 62 % of TFA in the mesocosms and between 48 % and 62 % in females collected in the adjacent Pacific. Both species had lower portions of SFAs than PUFAs contributing between 32 % and 48 % of TFA in copepods of the mesocoms and 32–40 % in those collected in the Pacific. At all times, FAlcs comprised less than 2 % of TFA indicating that these females of both genera did not accumulate significant amounts of wax esters (storage lipids).

3.5   Food web relationships

Pearson correlations (data not shown) revealed no particularly strong relationships between protist groups (diatoms, phytoflagellates, coccolithophores, dinoflagellates, silicoflagellates, Chloro-, Dino-, Crypto-, Prymnesio-, and Pelagophyceae, *Synechococcus)* and adult and copepodite stages of the copepods *Paracalanus* sp. and *Hemicyclops* sp.. The majority of correlations with a higher correlation coefficient were influenced by a single value, thus, we do not consider these correlations meaningful, in spite of their significance. Apart from that, no consistent associations were identified across the single mesocosms or the two OMZ treatments. Some more meaningful positive correlations were determined for both genera with Pelagophyceae, silicoflagellates, total Chl *a*, Cryptophyceae, and Chlorophyceae (p <0.05, Table S1). More conclusive negative correlations existed with dinoflagellates and Prymnesiophyceae. However, none of these correlations were consistent in all mesocosms,
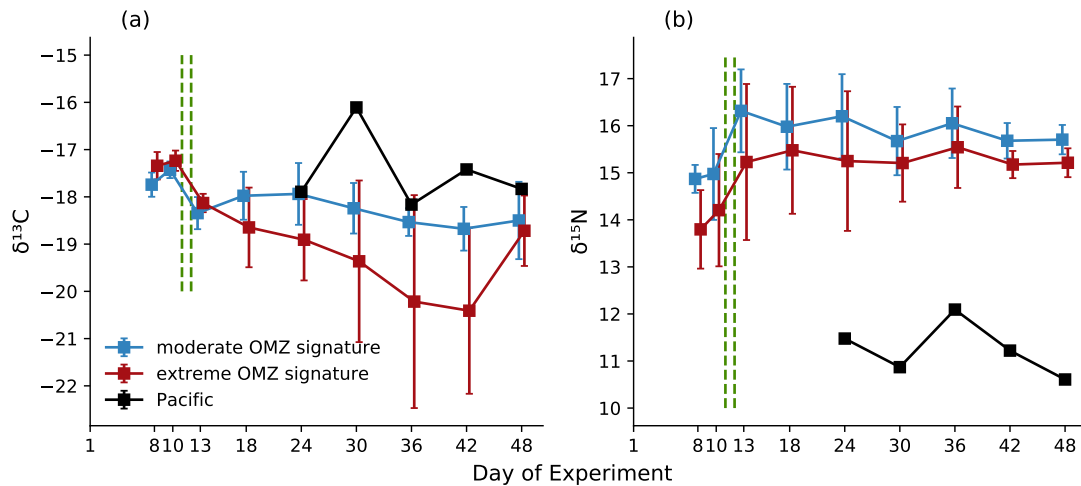
Figure 9. Temporal development averaged for the moderate and extreme treatments of δ^{13}C (a) and δ^{15}N (b) in copepods sampled in the eight mesocosms (M) and the adjacent Pacific (P). Error bars depict 95 % confidence intervals. The green vertical dashed lines indicate the days of OMZ water additions. The experimental phase 1 lasted from Day 1 until Day 11/12, phase 2 until Day 40, phase 3 until experiment termination.

470   i.e. we could not identify a consistent food web relation pattern for the dominant *Paracalanus* and *Hemicyclops* species in the different mesocosms. Apparently, these copepods fed very opportunistically with no major preference for any of the occurring protist groups. In the adjacent Pacific, positive correlations for *Paracalanus* sp. existed with silicoflagellates, Dinophyceae, Chlorophyceae and Chl *a* (p <0.05, Table S1).

3.6   Stable isotope and elemental composition

475   δ^{15}N and δ^{13}C values of copepods (bulk samples) were not impacted by treatment (except a marked difference in M4) (Table 1) but varied over time with a general increase in δ^{15}N and a decrease in δ^{13}C during the experimental period (Fig. 9).

During phase 1, δ^{15}N of copepods increased by ∼1 ‰ in all mesocosms, a further increase of 1 − 2 ‰ in δ^{15}N occurred during phase 2, while copepod δ^{15}N slightly decreased during phase 3. δ^{13}C was highest during phase 1 and fluctuated between phase 2 and 3. In mesocosm M4, the decrease in δ^{13}C was particularly pronounced. Generally, δ^{15}N values were substantially higher

480   and δ^{13}C values slightly lower in the mesocosms than in the copepods from the adjacent Pacific (Fig. 9). Copepod pooled C:N was unaffected by treatment, with an average value of 4.8 ($\pm$ 0.2), and ranged between 5.1 and 5.8 for *Hemicyclops* sp. and *Paracalanus* sp., respectively, based on species/genus-specific determinations. For the two polychaete species, temporal patterns of δ^{15}N and δ^{13}C values were difficult to resolve due to incomplete sampling, and did not reveal a consistent pattern (data available at PANGAEA, https://doi.org/10.1594/PANGAEA.947833, Lischka et al. (2022)). C:N ratios in the two polychaetes

485   were slightly lower than those of the copepods, with 4.3 ($\pm$ 0.44) and 4.2 ($\pm$ 0.44) in *Paraprionospio* sp. and *P. longicirrata*, respectively. DM-specific organic C, N and P contents were also lower in the two polychaetes than in the copepods. In all

Table 4. Mean and standard deviation (SD) of dry mass (DM), carbon, nitrogen and phosphorus content of dominant mesozooplankton taxa as well as their molar ratios.

Taxon	DM [μg Ind^{-1}]	C [μg mg^{-1} DM]	N [μg mg^{-1} DM]	P [μg mg^{-1} DM]	C:N (molar)	C:P (molar)	N:P (molar)
Copepods							
Copepods (pooled)	NA	338.4 (118.8)	82.9 (28.8)	4.09 (2.14)	4.8 (0.2)	214.4	45.0
Hemicyclops sp., CIV–CV (n=4)	2.2 (0.7)	313.9 (91)	66.5 (19.9)	NA	5.5 (0.15)	NA	NA
Hemicyclops sp., female (n=5)	4.5 (1.2)	404.1 (36.3)	81.1 (6.9)	NA	5.8 (0.11)	NA	NA
Paracalanus sp., CIV–CV (n=4)	3.3. (1.3)	234.4 (94.4)	52.2 (21.3)	NA	5.2 (0.26)	NA	NA
Paracalanus sp., female (n=7)	4.8 (1.7)	254.4 (55.6)	58.7 (13.4)	NA	5.1 (0.17)	NA	NA
Polychaets							
Paraprionospio sp.	Na	122.4 (69.6)	32.2 (16.2)	0.74 (1.05)	4.3 (0.44)	424.8	95.7
Pelagobia longicirrata	NA	117.6 (72)	32.4 (17.2)	1.30 (1.15)	4.4 (0.43)	232.2	53.3

mesozooplankton groups, C:P and N:P ratios were higher than 200 and 40, respectively (Table 4). While the analysis of parallel samples for C:N and P may explain part of the variability in the mesozooplankton, the comparatively low P content was also determined in the microzooplankton, where all elemental contents were analyzed per cell. We analyzed microzooplankton

490   cells of the genera *Dinophysis* cf. *punctata* (n = 127), *Tripos* (e.g. *T. fusus*, *T. furca*, n = 25), and *Protoperidinium* sp. (n = 3). In the analyzed dinoflagellates, cellular elemental ratios deviated even more from the canonical Redfield ratio (Table 5). Because the N:P additions in the different mesocosms were not very different, we pooled the analysis of microzooplankton per sampling day. Comparing single-cell analysis of *Dinophysis* cf. *punctata* from this study (Table 5) with the same taxa from the Mediterranean Sea, all species analyzed here had more C, N and O, but similar P contents (Segura-Noguera et al., 2016).

Table 5. Mean and standard deviation (SD) of cellular carbon, nitrogen, oxygen and phosphorus content of dominant microzooplankton taxa as well as their molar ratios.

Species	C [pg cell^{-1}]	N [pg cell^{-1}]	O [pg cell^{-1}]	P [pg cell^{-1}]	C:P (mean)	C:N (mean)	N:P (mean)	C:O (mean)
Ceratium furca	1209 (175)	155 (45)	1072 (316)	5.7 (3.7)	1076.9	9.7	110.4	1.6
Ceratium fusus sp.	1097 (305)	125 (33)	874 (229)	6.5 (2.1)	518.6	10.2	50.4	1.7
Ceratium sp.	2050 (380)	266 (61)	1881 (378)	14.0 (5.2)	453.3	9.2	49.0	1.5
Dinophysis cf. *punctata*	2172 (965)	208 (68)	1460 (463)	9.9 (4.9)	714.3	12.2	61.4	2.0
Protoperidinium sp.	1455 (450)	127 (125)	808 (798)	10.4 (9.3)	502.0	20.2	26.2	3.6

4 Discussion

4.1 Mesozooplankton dynamics

Our experiment coincided with a concurrent strong coastal El Niño, a situation of generally warmer waters and weaker up-welling conditions that favour small-sized zooplankton occurrence in the coastal upwelling areas (Ayón et al., 2011; Bertrand et al., 2011), and consequently dominated our mesozooplankton community in the mesocosm bags at the start of the experiment. The MeZP community comprised various taxonomic groups with copepods dominating throughout the experiment both in the mesocosms and the surrounding Pacific, therefore we focus our discussion on copepods. The four main genera were *Paracalanus*, *Hemicyclops*, *Acartia* and *Oncaea*. Species of the genus *Paracalanus*, *Acartia* and *Oncaea* are common in Peruvian coastal and neritic waters (e.g. Ayón et al., 2008a; Aronés et al., 2009; Ayón et al., 2011), whereas the occurrence of the cyclopoid copepod *Hemicyclops* sp. off Callao has only been reported by Criales-Hernández et al. (2008). During our study, *Hemicyclops* sp. regularly occurred in the surrounding Pacific with different developmental stages including older copepodids.

The observed developmental delay of copepodids and adults and especially the very low abundance of nauplii may be a consequence of hypoxic conditions in the mesocosms below ∼10 m. Copepod nauplii were rare in the mesocosms, particularly after deep-water addition between Day 18 and Day 30 (<1 % or absent), although females of the sac-spawning *Hemicyclops* and also the less abundant *Oncaea* were frequently observed carrying egg sacs (personal observations). In contrast, except for the first days of the experiment, nauplii almost consistently comprised around 20 % of all copepod stages in the surrounding Pacific until Day 30 and reached almost 80 % on Day 36. This could be explained by advection of copepod populations carrying higher numbers of nauplii (Ayón et al., 2008b) or turbulence/upwelling keeping eggs in the oxygenated layer and promoting hatching. A lack of nauplii is also reflected in the development of copepodids and adults over the experimental duration and is particularly evident for *Acartia* sp. with adult copepods dominating the population almost over the entire study period. Despite species-specific tolerance levels, copepods generally respond to hypoxic conditions with avoidance (adults) and decreasing rates of survival, egg production and population growth resulting in significant effects on population dynamics (e.g. Judkins, 1980; Marcus et al., 2004; Richmond et al., 2006; Ruz et al., 2017).

Eggs of *Paracalanus* sp., the dominant broadcast spawning (i.e. eggs released freely into the water column) copepod in the mesocosms, were probably particularly affected by hypoxia, when sinking into low oxygen waters. Field studies showed, maximum abundances of *Paracalanus* cf. *indicus* eggs in Mejillones Bay, Chile, were found in the oxygenated surface waters, whereas egg abundance decreased significantly from the oxygenated layer and the oxycline to the OMZ (Ruz et al., 2017). Sublethal and lethal hypoxia levels (<67 and <31 μmol L^{-1} O$_2$, respectively, Auel and Verheye (2007); Richmond et al. (2006)) occurred in all mesocosms and the surrounding Pacific consistently throughout the study, where the oxycline was between 5 and 15 m and dissolved oxygen concentrations decreased at depth to <50 μmol L^{-1} (Bach et al., 2020). Sinking velocities of *Paracalanus parvus* eggs determined in the lab and of *P.* cf. *indicus* determined in the field (Mejillones Bay, Chile) ranged between 2.4–16.9 m d^{-1} (Checkley, 1980a; Ruz et al., 2017). At a temperature range of 18–20° C, *P. parvus* nauplii hatch within 0.40 – 0.46 days and the generation time of *Paracalanus* is about 18 days at 18° C (Checkley, 1980a). During our study, due to the coastal El Niño, surface temperatures usually varied between 20° C and 22° C, exceptionally reaching 24° C between Day

14 and Day 22. Averaged over the entire mesocosm water column and all mesocosms, temperatures ranged between 18.4° C

530   and 20.2° C from Days 1 to 38 and between 17.9° C and 18.6° C thereafter (Bach et al., 2020). Thus, the experimental duration was long enough to expect *Paracalanus* eggs in the mesocosms. Eggs released at the mesocosms' surface would sink to 0.96–6.76 m depth within 0.4 days (= 9.6 h), respectively. Eggs released at greater depth would reach the oxycline and hypoxic layers faster, where development was likely halted or eggs may have suffered mortality. The accumulation of adults (respectively a minimum contribution of copepodids) around Day 24, after oxygen concentrations in the mesocosms had decreased below

535   50 μmol O$_2$ L^{-1} below 10 m depth (Bach et al., 2020) further supports our notion of hindered egg development due to hypoxic conditions.

A late increase in copepod nauplii discernible in the mesocosm treatments on Day 36 (extreme) and Day 42 (moderate) might have resulted from a co-occurring deepening of hypoxic layers (<55 μmol L^{-1}) from ~10 m to 14 – 15 m and slightly higher oxygen concentrations resulting from a phytoplankton bloom event facilitated through guanotrophication (Bach et al.,

540   2020). Similarly, a short intrusion of oxygen-richer waters up to ~10 m occurred in the adjacent Pacific, parallel to the small nauplii increase on Day 30. Together with the concomitant increase in food availability this may have supported an increase in eggs and nauplii in both mesocosm treatments.

Upwelling is an important factor shaping copepod population dynamics operating through an optimal window of upwelling intensity that fosters copepod abundance and biomass, whereas increasing upwelling may be unfavorable for copepod popula-

545   tions' (Escribano et al., 2012). This is in close connection with the fact that especially smaller copepods such as *Paracalanus* and *Acartia* require well-oxygenated waters for egg development and survival of early-stage copepods for population success (Ruz et al., 2017). Hence, our findings of failed egg/nauplii development strongly support these earlier notions and underline the importance of mesoscale variability and its implications for copepod reproduction in oxygenated waters and upwelling events, respectively.

550   ## 4.2   Trophic relations

Exhausted inorganic nitrogen sources and the dominance of the mixotrophic and facultative osmotrophic dinoflagellate *Akashiwo sanguinea* in the phytoplankton community in most mesocosms (absent in M4) seems the most likely reason for the extremely low GF of *Paracalanus* females during phase 2 of the experiment. Pigment contents determined for *Paracalanus* in our study were mostly an order of magnitude lower than those of *Acartia*, *Pseudocalanus* and *Temora* from Danish waters

555   (Kiørboe et al., 1985) and of *Acartia* off southern California (Kleppel et al., 1988). *Paracalanus parvus* prefers phytoplankton >5 μm over particulate matter as food source, but may also feed on dinoflagellates, when these dominate phytoplankton biomass (Checkley, 1980a; Kleppel and Pieper, 1984). Furthermore, visual inspection of guts of *Paracalanus* females revealed that guts were often empty and that they were not feeding directly on phytoplankton.

The low GF is in accordance with the very low occurrence or absence of phytoplankton biomarker fatty acids determined in

560   *Paracalanus* and *Hemicyclops* females in this study, and together point to the fact that development of these copepods depends on immediate food supply. Due to their very low lipid (TFA) levels, the fatty acid signatures of the copepods analyzed were largely dominated by biomembrane fatty acids (phospholipids), e.g. 16:0, 20:5(n-3) and 22:6(n-3). However, dietary signals of

marker fatty acids are conserved in the storage lipids, i.e., in wax esters or triacylglycerols (Lee et al., 2006; Dalsgaard et al., 2003). The marker fatty acid 16:1(n-7) typical of diatoms decreased in *Paracalanus* females from initially ca. 5 % to 1–2%

565 TFA in phase 3, suggesting diatom ingestion only before or at the beginning of the experiment. However, *Paracalanus* females collected in the adjacent Pacific during phase 3 had higher 16:1(n-7) concentrations of 10% indicative of diatom feeding in the wild. In contrast, the fatty acid 18:4(n-3) typical of flagellates was not detected in significant amounts in any of the copepods. The near absence of wax esters (storage lipid) agrees with previous studies that egg production in the studied species is related to immediate food supply rather than a period prior to actual egg production, when energy reserves may have been accumulated

570 (Checkley, 1980b).

Moreover, of the detected gut fluorescence no clear phaeopigment peaks were identifiable with HPLC, which points to a high degree of degradation of fluorescent pigments found in the guts. Possibly, this 'aged' gut fluorescence originated from ingestion of particulate matter, which could also explain why no particularly strong correlations existed between any of the phytoplankton groups and female abundance. The *A. sanguinea* bloom was associated with a marked increase of particulate

575 organic matter and of the C:N ratio (from about 5–6 to 8–12) in the water column of most mesocosms (Bach et al., 2020). However, phytoplankton availability, respectively dietary nitrogen (i.e. protein), is at times the direct limiting nutrient for egg production of *Paracalanus* (Checkley, 1980b). Hence, nutritional conditions for *Paracalanus* females were apparently insufficient in the mesocosms during phase 2, leading to low egg production and explaining the low numbers of nauplii found in the mesosocoms.

580 Like *Paracalanus*, *Hemicyclops*, may have lived at suboptimal conditions. Gut fluorescence was not detected in *Hemicylops* sp. The fatty acid composition of *Hemicyclops* females was analyzed only from Day 30 onwards and was very similar to that determined for *Paracalanus*. Except for very low concentrations (2–3 % TFA) of the diatom marker 16:1(n-7), no trophic marker fatty acids were identified and no fatty alcohols were determined, hence, no wax esters (storage lipid) were present. Correlation analysis suggested no particular food preference of *Hemicyclops* for any of the prevailing phytoplankton groups.

585 The diet of *Hemicyclops* species with a coupled pelagic-benthic life cycle consists of micro- and meiobenthos, while detrital particles and also bacteria might be additional food sources (Itoh and Nishida, 2007, and references therein). Unfortunately, no studies are available on food preferences of *H. thalassius*. Although *Hemicyclops* is an egg-sac spawner, virtually no nauplii were found over the experimental runtime. Using a 100 μm mesh net, we may have missed the younger nauplii, but should have captured the older naupliar stages (Itoh and Nishida, 2008). From the absence of nauplii despite the frequent presence

590 of egg-sac carrying females, we conclude that the *Hemicyclops* populations in the mesocosms, like *Paracalanus*, also lived at suboptimal conditions, both in terms of nutrition and dissolved oxygen concentrations.

Isotopic signatures of zooplankton are determined by source and trophic fractionation. The latter is particularly the case for δ^{15}N, where an increase of $3-4$‰ per trophic level is usually assumed for marine food webs (Cabana and Rasmussen, 1994; Minagawa and Wada, 1984; Peterson and Fry, 1987). Zooplankton δ^{15}N values ranging approximately between 5 and

595 13‰ occur in (and close to) upwelling areas (e.g. Rau et al., 2003; Schukat et al., 2014; Teuber et al., 2014), whereas lower zooplankton δ^{15}N values ($\sim 2-4$‰) were found in regions with high diazotroph contribution to the pelagic food web (Hauss et al., 2013; Sandel et al., 2015). δ^{15}N of zooplankton (copepods) in the mesocosms following a simulated upwelling pulse were

rather high ($\sim 13 - 17\,\%o$) as compared to the δ^{15}N (mean 7.6 ‰) measured by Espinoza et al. (2017) for bulk copepod samples of the HCS. The δ^{13}C ratio of copepods from M4 differed profoundly from the other mesocosms in phase 2 (Day 13 – 36). The decrease in δ^{13}C seems to correlate with an increase of Chlorophyceae which made up >90 % of the phytoplankton community on Day 36 (Bach et al., 2020). Turnover time of δ^{13}C in copepods varies from days to weeks (Gentsch et al., 2008). An increase of Chlorophyceae and following constant supply should be seen in the C signal of the copepods after several days. Also, in contrast to the other mesocosms, δ^{15}N was generally lower in M4 in the first two phases. M4 was the only mesocosm lacking the dinoflagellate *Akashiwo sanguinea* (Bach et al., 2020). Mixotrophy by this flagellate could thus have led to increased nitrogen fractionation in the other mesocosms. A comparison of δ^{15}N among different studies without clearly defined baseline values (phytoplankton) for comparison is difficult, as the δ^{15}N baseline is strongly affected by the variability in the intensity of the OMZ along the Peruvian coast (Mollier-Vogel et al., 2012). A recent study by Massing et al. (2022) revealed an enrichment in δ^{15}N of $\sim 5\,\%o$ for several copepod species of the HCS from north (8.5° S) to south (16° S). The δ^{15}N ratios of seston also increased with depth, i.e. between seston from surface oxygenated waters and the OMZ. Dissolved inorganic nitrogen taken up by phytoplankton often creates the basis of the isotopic composition of the whole food web (Argüelles et al., 2012). Under anoxic conditions in OMZs, a preferred uptake of the lighter isotope by denitrifiers leads to elevated δ^{15}N in the remaining nitrate (Granger et al., 2008). OMZs such as the strong and shallow one in the northern HCS are, thus, sites of intense nitrogen loss (Ward et al., 1989) leading to an increase in δ^{15}N baseline values (Sigman et al., 1999; Graham et al., 2010). The higher δ^{15}N of copepods within the mesocosms can therefore be a result of/may be explained by the source water injection to the mesocosms, which was reduced in oxygen and most likely enriched in δ^{15}N. Starvation would lead to loss of body mass and preferential metabolism of the lighter isotope, with a resulting increase in delta values for both tracers (Hobson et al., 1993; Gannes et al., 1997).

5   Conclusions

Our results provide interesting insight on the response of a zooplankton community and their trophic relations to an upwelling event with OMZ waters. In particular GF and fatty acid compositions revealed that after deep-water addition feeding of dominant copepods on autotrophic food (diatoms) was insignificant and copepods lived from "hand to mouth". This may point to an important role of hetero-/mixotrophic organisms as food source for copepods. Though egg production was not determined in our study, we assume, the lack of nauplii during most of the experiment duration was preceded by failed production and/or development of copepod eggs and nauplii, both due to prevailing hypoxic and insufficient nutritional conditions in the mesocosms. With respect to hypoxia, we conclude a few meters of oxygenated waters more or less may make a huge difference for copepod secondary production. With respect to nutrition, changing N:P ratios of upwelled water may further contribute to negatively impact copepod reproductive success, as the availability of nitrogen-rich food sources is important for reproductive output of copepods relying on immediate food supply for egg production (Checkley, 1980b). Hence, increasing upwelling intensity and shoaling of the OMZ as projected for EBUS under ocean warming (Stramma et al., 2008; Schmidtko et al., 2017) may have severe consequences for mesopelagic food webs, trophic transfer, and fish production in the HUS (Ayón

et al., 2008b; Aronés et al., 2019). Perspectively, future studies should focus on the nutritional condition and fecundity of the copepods, the importance of heterotrophic food sources in the nutrition of copepods, and of microzooplankton grazing in the food web. Measures of nutritional condition would also help to strengthen interpretation of isotopic signatures in relation to starvation of organisms. Together this would add further detail to a more comprehensive understanding of the response of plankton communities and their trophic links to the projected varying impact of upwelling intensity and/or frequency of OMZ waters off Peru.

635

Data availability. All data will be made available on the permanent repository www.pangaea.de after publication. Publication and usage of these data with respect to access and benefit sharing regulations under the Nagoya protocol were approved by the Peruvian Ministry of Production (PRODUCE).

640 *Author contributions.* PA, SL, AS, RK, and JT designed the experiment. AS, SL, JT, EP, PA, and RK contributed to the MeZP and MiZP sampling. PA and EP performed MeZP abundance determinations. SL and PA analyzed MeZP abundance data, SL performed correlation analysis and rmANOVA. SL collected samples for copepod gut fluorescence, performed analyses, and analyzed data. SL and AS picked copepods for fatty acid analyses, WH and SD performed fatty acid analyses, SL, AS, WH, and SD analyzed fatty acid data. AS performed sampling for SI determinations of MeZP and elemental composition of MiZP, and together with HH and MS-N analyzed the data. JT and RK 645 performed ZooScan analysis, HH analyzed ZooScan data and calculated biomass. SL wrote the manuscript with input from all co-authors.

Competing interests. The authors declare that they have no conflict of interests.

Acknowledgements. We thank all participants of the KOSMOS Peru 2017 study for assisting in mesocosm sampling and maintenance. We are especially grateful to the IMARPE staff for all support from planning of the study to execution. The captains and crews of BAP Morales, IMARPE VI, and BIC Humboldt are gratefully acknowledged for support during deployment and recovery of the mesocosms and 650 various operations during the course of this investigation. Special thanks go to the Marina de Guerra del Perú, in particular the submarine section of the navy of Callao, and to the Dirección General de Capitanías y Guardacostas. We also thank Club Náutico Del Centro Naval for hosting and providing laboratory facilities. Our colleagues Clara Beckmann, Jean-Pierre Bednar, Tim Boxhammer, Svenja Christiansen, Lara Durchgraf, Jannik Faustmann, Alba Filella, Marcello Muñiz, Kerstin Nachtigall, Claudia Sforna, Ulf Riebesell, Roberto Quesquén, Laura Schütt, Carsten Spisla, Mayte Tames-Espinosa, Nele Weigt, and Mabel Zavala Moreira are acknowledged for their valuable support 655 during sampling, processing and analyses of zooplankton samples. This project was supported by the Collaborative Research Centre SFB 754 Climate-Biogeochemistry Interactions in the Tropical Ocean financed by the German Research Foundation (DFG). Additional funding was provided through the Leibniz Award 2012 granted to Ulf Riebesell. This work is a contribution in the framework of the cooperation agreement between IMARPE and GEOMAR through the German Federal Ministry of Education and Research (BMBF) project ASLAEL 12-016 and the national project Integrated Study of the Upwelling System off Peru developed by the Directorate of Oceanography and

660   Climate Change of IMARPE, PPR 137 CONCYTEC. Rainer Kiko, Silke Lischka, and Helena Hauss received support by the CUSCO project (Bundesministerium für Bildung und Forschung grant no. 03F0813A). Rainer Kiko was further supported via a Make Our Planet Great Again grant of the French National Research Agency within the Programme d'Investissements d'Avenir, reference ANR-19-MPGA-0012.

References

Alguero-Muñiz, M., Alvarez-Fernandez, S., Thor, P., Bach, L. T., Esposito, M., Horn, H. G., Ecker, U., Langer, J. A. F., Taucher, J., Malzahn, A. M., Riebesell, U., and Boersma, M.: Ocean acidification effects on mesozooplankton community development: Results from a long-term mesocosm experiment, PLOS ONE, 12, 1–21, https://doi.org/10.1371/journal.pone.0175851, 2017.

Argüelles, J., Lorrain, A., Cherel, Y., Graco, M., Tafur, R., Alegre, A., Espinoza, P., Taipe, A., Ayón, P., and Bertrand, A.: Tracking habitat and resource use for the jumbo squid *Dosidicus gigas*: a stable isotope analysis in the Northern Humboldt Current System, Marine Biology, 159, 2105–2116, https://doi.org/10.1007/s00227-012-1998-2, 2012.

Arones, K., Grados, D., Ayón, P., and Bertrand, A.: Spatio-temporal trends in zooplankton biomass in the northern Humboldt current system off Peru from 1961-2012, Deep Sea Research Part II: Topical Studies in Oceanography, 169-170, 104 656, https://doi.org/10.1016/j.dsr2.2019.104656, 2019.

Arones, K., Ayón, P., Hirche, H.-J., and Schwamborn, R.: Hydrographic structure and zooplankton abundance and diversity off Paita, northern Peru (1994 to 2004) — ENSO effects, trends and changes, Journal of Marine Systems, 78, 582–598, https://doi.org/10.1016/j.jmarsys.2009.01.002, revisiting the Role of Zooplankton in Pelagic Ecosystems, 2009.

Auel, H. and Verheye, H. M.: Hypoxia tolerance in the copepod *Calanoides carinatus* and the effect of an intermediate oxygen minimum layer on copepod vertical distribution in the northern Benguela Current upwelling system and the Angola-Benguela Front, Journal of Experimental Marine Biology and Ecology, 352, 234–243, https://doi.org/10.1016/j.jembe.2007.07.020, 2007.

Ayón, P., Criales-Hernandez, M. I., Schwamborn, R., and Hirche, H.-J.: Zooplankton research off Peru: A review, Progress in Oceanography, 79, 238–255, https://doi.org/10.1016/j.pocean.2008.10.020, 2008a.

Ayón, P., Swartzman, G., Bertrand, A., Gutiérrez, M., and Bertrand, S.: Zooplankton and forage fish species off Peru: Large-scale bottom-up forcing and local-scale depletion, Progress in Oceanography, 79, 208–214, https://doi.org/10.1016/j.pocean.2008.10.023, 2008b.

Ayón, P., Swartzman, G., Espinoza, P., and Bertrand, A.: Long-term changes in zooplankton size distribution in the Peruvian Humboldt Current System: conditions favouring sardine or anchovy, Marine Ecology Progress Series, 422, 211–222, https://www.int-res.com/abstracts/meps/v422/p211-222/, 2011.

Bach, L. T., Boxhammer, T., Larsen, A., Hildebrandt, N., Schulz, K. G., and Riebesell, U.: Influence of plankton community structure on the sinking velocity of marine aggregates, Global Biogeochemical Cycles, 30, 1145–1165, https://doi.org/https://doi.org/10.1002/2016GB005372, 2016.

Bach, L. T., Paul, A. J., Boxhammer, T., von der Esch, E., Graco, M., Schulz, K. G., Achterberg, E., Aguayo, P., Arístegui, J., Ayón, P., Baños, I., Bernales, A., Boegeholz, A. S., Chavez, F., Chavez, G., Chen, S.-M., Doering, K., Filella, A., Fischer, M., Grasse, P., Haunost, M., Hennke, J., Hernández-Hernández, N., Hopwood, M., Igarza, M., Kalter, V., Kittu, L., Kohnert, P., Ledesma, J., Lieberum, C., Lischka, S., Löscher, C., Ludwig, A., Mendoza, U., Meyer, J., Meyer, J., Minutolo, F., Ortiz Cortes, J., Piiparinen, J., Sforna, C., Spilling, K., Sanchez, S., Spisla, C., Sswat, M., Zavala Moreira, M., and Riebesell, U.: Factors controlling plankton community production, export flux, and particulate matter stoichiometry in the coastal upwelling system off Peru, Biogeosciences, 17, 4831–4852, https://doi.org/10.5194/bg-17-4831-2020, 2020.

Bakun, A. and Weeks, S. J.: The marine ecosystem off Peru: What are the secrets of its fishery productivity and what might its future hold?, Progress in Oceanography, 79, 290–299, https://doi.org/10.1016/j.pocean.2008.10.027, 2008.

Båmstedt, U., Gifford, D., Irigoien, X., Atkinson, A., and Roman, M.: 8 - Feeding, in: ICES Zooplankton Methodology Manual, edited by Harris, R., Wiebe, P., Lenz, J., Skjoldal, H. R., and Huntley, M., pp. 297–399, Academic Press, London, https://doi.org/10.1016/B978-012327645-2/50009-8, 2000.

Barlow, R. G., Cummings, D. G., and Gibb, S. W.: Improved resolution of mono- and divinyl chlorophylls a and b and zeaxanthin and lutein in phytoplankton extracts using reverse phase C-8 HPLC, Marine Ecology Progress Series, 161, 303–307, http://www.int-res.com/abstracts/meps/v161/p303-307/, 1997.

Bertrand, A., Chaigneau, A., Peraltilla, S., Ledesma, J., Graco, M., Monetti, F., and Chavez, F. P.: Oxygen: A Fundamental Property Regulating Pelagic Ecosystem Structure in the Coastal Southeastern Tropical Pacific, PLOS ONE, 6, 1–8, https://doi.org/10.1371/journal.pone.0029558, 2011.

Cabana, G. and Rasmussen, J. B.: Modelling food chain structure and contaminant bioaccumulation using stable nitrogen isotopes, Nature, 372, 255–257, https://doi.org/10.1038/372255a0, 1994.

Carr, M.-E.: Estimation of potential productivity in Eastern Boundary Currents using remote sensing, Deep Sea Research Part II: Topical Studies in Oceanography, 49, 59–80, https://doi.org/10.1016/S0967-0645(01)00094-7, 2001.

Chavez, F. P. and Messié, M.: A comparison of Eastern Boundary Upwelling Ecosystems, Progress in Oceanography, 83, 80–96, https://doi.org/10.1016/j.pocean.2009.07.032, 2009.

Chavez, F. P., Bertrand, A., Guevara-Carrasco, R., Soler, P., and Csirke, J.: The northern Humboldt Current System: Brief history, present status and a view towards the future, Progress in Oceanography, 79, 95–105, https://doi.org/10.1016/j.pocean.2008.10.012, 2008.

Checkley, D. M.: Food limitation of egg production by a marine, planktonic copepod in the sea off southern California, Limnology and Oceanography, 25, 991–998, https://doi.org/10.4319/lo.1980.25.6.0991, 1980a.

Checkley, D. M.: The egg production of a marine planktonic copepod in relation to its food supply: Laboratory studies, Limnology and Oceanography, 25, 430–446, https://doi.org/10.4319/lo.1980.25.3.0430, 1980b.

Criales-Hernández, M. I., Schwamborn, R., Graco, M., Ayón, P., Hirche, H. J., and Wolff, M.: Zooplankton vertical distribution and migration off Central Peru in relation to the oxygen minimum layer, Helgoland Marine Research, 62, 85–100, https://doi.org/10.1007/s10152-007-0094-3, 2008.

Cullen, J. J., Lewis, M. R., Davis, C. O., and Barber, R. T.: Photosynthetic characteristics and estimated growth rates indicate grazing is the proximate control of primary production in the equatorial Pacific, Journal of Geophysical Research, 97, 639–654, https://doi.org/10.1029/91JC01320, 1992.

Dalsgaard, J., St John, M., Kattner, G., Müller-Navarra, D., and Hagen, W.: Fatty acid trophic markers in the pelagic marine environment., Adv Mar Biol, 46, 225–340, https://doi.org/10.1016/s0065-2881(03)46005-7, 2003.

Ehrhardt, M. and Koeve, W.: Determination of particulate organic carbon and nitrogen, chap. 17, pp. 437–444, John Wiley and Sons, Ltd, https://doi.org/10.1002/9783527613984.ch17, 1999.

Escribano, R.: Population dynamics of *Calanus chilensis* in the Chilean Eastern Boundary Humboldt Current, Fisheries Oceanography, 7, 245–251, https://doi.org/10.1046/j.1365-2419.1998.00078.x, 1998.

Escribano, R., Hidalgo, P., Fuentes, M., and Donoso, K.: Zooplankton time series in the coastal zone off Chile: Variation in upwelling and responses of the copepod community, Progress in Oceanography, 97-100, 174–186, https://doi.org/10.1016/j.pocean.2011.11.006, global Comparisons of Zooplankton Time Series, 2012.

Espinoza, P. and Bertrand, A.: Revisiting Peruvian anchovy (*Engraulis ringens*) trophodynamics provides a new vision of the Humboldt Current system, Progress in Oceanography, 79, 215–227, https://doi.org/10.1016/j.pocean.2008.10.022, 2008.

Espinoza, P. and Bertrand, A.: Ontogenetic and spatiotemporal variability in anchoveta *Engraulis ringens* diet off Peru, Journal of Fish Biology, 84, 422–435, https://doi.org/10.1111/jfb.12293, 2014.

Espinoza, P., Bertrand, A., van der Lingen, C. D., Garrido, S., and Rojas de Mendiola, B.: Diet of sardine (*Sardinops sagax*) in the northern Humboldt Current system and comparison with the diets of clupeoids in this and other eastern boundary upwelling systems, Progress in Oceanography, 83, 242–250, https://doi.org/10.1016/j.pocean.2009.07.045, 2009.

Espinoza, P., Lorrain, A., Ménard, F., Cherel, Y., Tremblay-Boyer, L., Argüelles, J., Tafur, R., Bertrand, S., Tremblay, Y., Ayón, P., Munaron, J. M., Richard, P., and Bertrand, A.: Trophic structure in the northern Humboldt Current system: new perspectives from stable isotope analysis, Marine Biology, 164, 86, https://doi.org/10.1007/s00227-017-3119-8, 2017.

Field, A., Miles, J., and Fields, Z., eds.: Discovering Statistics using R, Sage Publications, Ltd, 2012.

Folch, J., Lees, M. B., and Stanley, G.: A simple method for the isolation and purification of total lipids from animal tissues., The Journal of biological chemistry, 226 1, 497–509, 1957.

Franz, J., Krahmann, G., Lavik, G., Grasse, P., Dittmar, T., and Riebesell, U.: Dynamics and stoichiometry of nutrients and phytoplankton in waters influenced by the oxygen minimum zone in the eastern tropical Pacific, Deep Sea Research Part I: Oceanographic Research Papers, 62, 20–31, https://doi.org/10.1016/j.dsr.2011.12.004, 2012a.

Franz, J. M. S., Hauss, H., Sommer, U., Dittmar, T., and Riebesell, U.: Production, partitioning and stoichiometry of organic matter under variable nutrient supply during mesocosm experiments in the tropical Pacific and Atlantic Ocean, Biogeosciences, 9, 4629–4643, https://doi.org/10.5194/bg-9-4629-2012, 2012b.

Gannes, L. Z., O'Brien, D. M., and del Rio, C. M.: STABLE ISOTOPES IN ANIMAL ECOLOGY: ASSUMPTIONS, CAVEATS, AND A CALL FOR MORE LABORATORY EXPERIMENTS, Ecology, 78, 1271–1276, https://doi.org/https://doi.org/10.1890/0012-9658(1997)078[1271:SIIAEA]2.0.CO;2, 1997.

García-Reyes, M., Sydeman, W. J., Schoeman, D. S., Rykaczewski, R. R., Black, B. A., Smit, A. J., and Bograd, S. J.: Under Pressure: Climate Change, Upwelling, and Eastern Boundary Upwelling Ecosystems, Frontiers in Marine Science, 2, 109, https://doi.org/10.3389/fmars.2015.00109, 2015.

Gentsch, E., Kreibich, T., Hagen, W., and Niehoff, B.: Dietary shifts in the copepod Temora longicornis during spring: evidence from stable isotope signatures, fatty acid biomarkers and feeding experiments, Journal of Plankton Research, 31, 45–60, https://doi.org/10.1093/plankt/fbn097, 2008.

Gorsky, G., Ohman, M. D., Picheral, M., Gasparini, S., Stemmann, L., Romagnan, J.-B., Cawood, A., Pesant, S., García-Comas, C., and Prejger, F.: Digital zooplankton image analysis using the ZooScan integrated system, Journal of Plankton Research, 32, 285–303, https://doi.org/10.1093/plankt/fbp124, 2010.

Graco, M. I., Purca, S., Dewitte, B., Castro, C. G., Morón, O., Ledesma, J., Flores, G., and Gutiérrez, D.: The OMZ and nutrient features as a signature of interannual and low-frequency variability in the Peruvian upwelling system, Biogeosciences, 14, 4601–4617, https://doi.org/10.5194/bg-14-4601-2017, 2017.

Graham, B., Koch, P., Newsome, S., McMahon, K., and Aurioles, D.: Using isoscapes to trace the movements and foraging behavior of top predators in oceanic ecosystems, in: Isoscapes: Understanding movement, pattern, and process on Earth through isotope mapping, edited by West, J., Bowen, G., Dawson, T., and Tu, K., pp. 299–318, Springer Netherlands, Dordrecht, 2010.

Granger, J., Sigman, D. M., Lehmann, M. F., and Tortell, P. D.: Nitrogen and oxygen isotope fractionation during dissimilatory nitrate reduction by denitrifying bacteria, Limnology and Oceanography, 53, 2533–2545, https://doi.org/10.4319/lo.2008.53.6.2533, 2008.

Gruber, N., Hauri, C., Lachkar, Z., Loher, D., Frölicher, T. L., and Plattner, G. K.: Rapid progression of ocean acidification in the California Current System, Science, 337, 220–223, https://doi.org/10.1126/science.1216773, 2012.

775 Hagen, W.: ICES Zooplankton Methodology Manual, Elsevier, San Diego, https://doi.org/10.1016/B978-0-12-327645-2.X5000-2, 2000.

Hauss, H., Franz, J. M. S., and Sommer, U.: Changes in N:P stoichiometry influence taxonomic composition and nutritional quality of phytoplankton in the Peruvian upwelling, Journal of Sea Research, 73, 74–85, https://doi.org/10.1016/j.seares.2012.06.010, 2012.

Hauss, H., Franz, J. M., Hansen, T., Struck, U., and Sommer, U.: Relative inputs of upwelled and atmospheric nitrogen to the eastern tropical North Atlantic food web: Spatial distribution of δ^{15}N in mesozooplankton and relation to dissolved nutrient dynamics, Deep Sea Research

780 Part I: Oceanographic Research Papers, 75, 135–145, https://doi.org/10.1016/j.dsr.2013.01.010, 2013.

Hobson, K. A., Alisauskas, R. T., and Clark, R. G.: Stable-Nitrogen Isotope Enrichment in Avian Tissues Due to Fasting and Nutritional Stress: Implications for Isotopic Analyses of Diet, The Condor, 95, 388–394, https://doi.org/10.2307/1369361, 1993.

Ingall, E. and Jahnke, R.: Evidence for enhanced phosphorus regeneration from marine sediments overlain by oxygen depleted waters, Geochimica et Cosmochimica Acta, 58, 2571–2575, https://doi.org/10.1016/0016-7037(94)90033-7, 1994.

785 Itoh, H. and Nishida, S.: Life history of the copepod *Hemicyclops gomsoensis* (Poecilostomatoida, Clausidiidae) associated with decapod burrows in the Tama-River estuary, central Japan, Plankton and Benthos Research, 2, 134–146, https://doi.org/10.3800/pbr.2.134, 2007.

Itoh, H. and Nishida, S.: Life history of the copepod *Hemicyclops spinulosus* (Poecilostomatoida, Clausidiidae) associated with crab burrows with notes on male polymorphism and precopulatory mate guarding, Plankton and Benthos Research, 3, 189–201, https://doi.org/10.3800/pbr.3.189, 2008.

790 Judkins, D. C.: Vertical distribution of zooplankton in relation to the oxygen minimum off Peru, Deep Sea Research Part A. Oceanographic Research Papers, 27, 475–487, https://doi.org/10.1016/0198-0149(80)90057-6, 1980.

Kalvelage, T., Jensen, M. M., Contreras, S., Revsbech, N. P., Lam, P., Günter, M., LaRoche, J., Lavik, G., and Kuypers, M. M. M.: Oxygen Sensitivity of Anammox and Coupled N-Cycle Processes in Oxygen Minimum Zones, PLoS ONE, 6, e29 299, https://doi.org/10.1371/journal.pone.0029299, 2011.

795 Karl, D. M., Letelier, R., Hebel, D., Tupas, L., Dore, J., Christian, J., and Winn, C.: Ecosystem changes in the North Pacific subtropical gyre attributed to the 1991–92 El Niño, Nature, 373, 230–234, https://doi.org/10.1038/373230a0, 1995.

Kattner, G. and Fricke, H. S.: Simple gas-liquid chromatographic method for the simultaneous determination of fatty acids and alcohols in wax esters of marine organisms, Journal of Chromatography A, 361, 263 – 268, https://doi.org/10.1016/S0021-9673(01)86914-4, 1986.

Kiørboe, T., Møhlenberg, F., and Riisgård, H. U.: In situ feeding rates of plantonic copepods: A comparison of four methods, Journal of

800 Experimental Marine Biology and Ecology, 88, 67–81, https://doi.org/10.1016/0022-0981(85)90202-3, 1985.

Kleppel, G. S. and Pieper, R. E.: Phytoplankton pigments in the gut concents of planktonic copepods from coastal waters off southern California, Marine Biology, 78, 193–198, https://doi.org/10.1007/BF00394700, 1984.

Kleppel, G. S., Pieper, R. E., and Trager, G.: Variability in the gut contents of individual *Acartia tonsa* from waters off Southern California, Marine Biology, 97, 185–190, https://doi.org/10.1007/BF00391301, 1988.

805 Konchina, Y.: Trophic status of the Peruvian Anchovy and Sardine, Journal of Ichtyology, 31, 240–252, 1991.

Kudela, R. M., Seeyave, S., and Cochlan, W. P.: The role of nutrients in regulation and promotion of harmful algal blooms in upwelling systems, Progress in Oceanography, 85, 122–135, https://doi.org/10.1016/j.pocean.2010.02.008, 2010.

Lee, R., Hagen, W., and Kattner, G.: Lipid storage in marine zooplankton, Marine Ecology Progress Series, 307, 273–306, https://doi.org/10.3354/meps307273, 2006.

810 Lehette, P. and Hernández-León, S.: Zooplankton biomass estimation from digitized images: a comparison between subtropical and Antarctic organisms, Limnology and Oceanography: Methods, 7, 304–308, https://doi.org/10.4319/lom.2009.7.304, 2009.

Lischka, S. and Hagen, W.: Seasonal lipid dynamics of the copepods Pseudocalanus minutus (Calanoida) and Oithona similis (Cyclopoida) in the Arctic Kongsfjorden (Svalbard), Marine Biology, 150, 443–454, https://doi.org/10.1007/s00227-006-0359-4, 2007.

Lischka, S., Bach, L. T., Schulz, K.-G., and Riebesell, U.: Ciliate and mesozooplankton community response to increasing CO_2 levels in
815 the Baltic Sea: insights from a large-scale mesocosm experiment, Biogeosciences, 14, 447–466, https://doi.org/10.5194/bg-14-447-2017, 2017.

Lischka, S., Ayón, P., Pinedo Arteaga, E. L., Schukat, A., Taucher, J., Kiko, R., Hauss, H., Dorschner, S., Hagen, W., and Segura-Noguera, M.: Response of zooplankton community succession and trophic links to simulated upwelling conditions during a meso-cosm experiment in the coastal upwelling off Callao Bay (Peru) in austral summer 2017 (KOSMOS 2017 Peru mesocosm study),
820 https://doi.org/10.1594/PANGAEA.947833, 2022.

Löscher, C. R., Bange, H. W., Schmitz, R. A., Callbeck, C. M., Engel, A., Hauss, H., Kanzow, T., Kiko, R., Lavik, G., Loginova, A., Melzner, F., Meyer, J., Neulinger, S. C., Pahlow, M., Riebesell, U., Schunck, H., Thomsen, S., and Wagner, H.: Water column biogeochemistry of oxygen minimum zones in the eastern tropical North Atlantic and eastern tropical South Pacific oceans, Biogeosciences, 13, 3585–3606, https://doi.org/10.5194/bg-13-3585-2016, 2016.

825 Mackas, D. and Bohrer, R.: Fluorescence analysis of zooplankton gut contents and an investigation of diel feeding patterns, Journal of Experimental Marine Biology and Ecology, 25, 77–85, https://doi.org/10.1016/0022-0981(76)90077-0, 1976.

Marcus, N. H., Richmond, C., Sedlacek, C., Miller, G. A., and Oppert, C.: Impact of hypoxia on the survival, egg produc-tion and population dynamics of *Acartia tonsa* Dana, Journal of Experimental Marine Biology and Ecology, 301, 111–128, https://doi.org/10.1016/j.jembe.2003.09.016, 2004.

830 Massing, J. C., Schukat, A., Auel, H., Auch, D., Kittu, L., Pinedo Arteaga, E. L., Correa Acosta, J., and Hagen, W.: Toward a Solution of the "Peruvian Puzzle": Pelagic Food-Web Structure and Trophic Interactions in the Northern Humboldt Current Upwelling System Off Peru, Frontiers in Marine Science, 8, https://doi.org/10.3389/fmars.2021.759603, 2022.

Minagawa, M. and Wada, E.: Stepwise enrichment of $\delta^{15}N$ along food chains: Further evidence and the relation between $\delta^{15}N$ and animal age, Geochimica et Cosmochimica Acta, 48, 1135–1140, https://doi.org/10.1016/0016-7037(84)90204-7, 1984.

835 Minas, H. J., Minas, M., and Packard, T. T.: Productivity in upwelling areas deduced from hydrographic and chemical fields, Limnology and Oceanography, 31, 1182–1206, https://doi.org/10.4319/lo.1986.31.6.1182, 1986.

Mollier-Vogel, E., Ryabenko, E., Martinez, P., Wallace, D., Altabet, M. A., and Schneider, R.: Nitrogen isotope gradients off Peru and Ecuador related to upwelling, productivity, nutrient uptake and oxygen deficiency, Deep Sea Research Part I: Oceanographic Research Papers, 70, 14–25, https://doi.org/10.1016/j.dsr.2012.06.003, 2012.

840 Peters, J., Dutz, J., and Hagen, W.: Role of essential fatty acids on the reproductive success of the copepod *Temora longicornis* in the North Sea, Marine Ecology Progress Series, 341, 153–163, 2007.

Peterson, B. J. and Fry, B.: Stable isotopes in ecosystem studies, Annual Review of Ecology and Systematics, 18, 293–320, https://doi.org/10.1146/annurev.es.18.110187.001453, 1987.

Picheral, M., Colin, S., and Irisson, J.-O.: EcoTaxa, a tool for the taxonomic classification of images, http://ecotaxa.obs-vlfr.fr, 2017.

845 R Core Team: R: A Language and Environment for Statistical Computing, R Foundation for Statistical Computing, Vienna, Austria, http://www.R-project.org/, ISBN 3-900051-07-0, 2014.

Rau, G. H., Ohman, M. D., and Pierrot-Bults, A.: Linking nitrogen dynamics to climate variability off central California: a 51 year record based on $\delta^{15}N/\delta^{14}N$ in CalCOFI zooplankton, Deep Sea Research Part II: Topical Studies in Oceanography, 50, 2431–2447, https://doi.org/10.1016/S0967-0645(03)00128-0, 2003.

850 Richmond, C., Marcus, N. H., Sedlacek, C., Miller, G. A., and Oppert, C.: Hypoxia and seasonal temperature: Short-term effects and long-term implications for Acartia tonsa dana, Journal of Experimental Marine Biology and Ecology, 328, 177–196, https://doi.org/10.1016/j.jembe.2005.07.004, 2006.

Ruz, P., Hidalgo, P., Riquelme-Bugueño, R., Franco-Cisterna, B., and Cornejo, M.: Vertical distribution of copepod eggs in the oxygen minimum zone off Mejillones Bay (23°S) in the Humboldt Current System, Marine Ecology Progress Series, 571, 83–96, https://www.

855 int-res.com/abstracts/meps/v571/p83-96/, 2017.

Ryther, J. H.: Photosynthesis and Fish Production in the Sea, Science, 166, 72–76, https://doi.org/10.1126/science.166.3901.72, 1969.

Sandel, V., Kiko, R., Brandt, P., Dengler, M., Stemmann, L., Vandromme, P., Sommer, U., and Hauss, H.: Nitrogen Fuelling of the Pelagic Food Web of the Tropical Atlantic, PLOS ONE, 10, 1–19, https://doi.org/10.1371/journal.pone.0131258, 2015.

Schmidtko, S., Stramma, L., and Visbeck, M.: Decline in global oceanic oxygen content during the past five decades, Nature, 542, 335–339,

860 https://doi.org/10.1038/nature21399, 2017.

Schröder, S.-M., Kiko, R., and Koch, R.: MorphoCluster: Efficient Annotation of Plankton Images by Clustering, Sensors, 20, https://doi.org/10.3390/s20113060, 2020.

Schukat, A., Auel, H., Teuber, L., Lahajnar, N., and Hagen, W.: Complex trophic interactions of calanoid copepods in the Benguela upwelling system, Journal of Sea Research, 85, 186–196, https://doi.org/doi.org/10.1016/j.seares.2013.04.018, 2014.

865 Schwartzlose, R. A., Alheit, J., Bakun, A., Baumgartner, T. R., Cloete, R., Crawford, R. J., Fletcher, W. J., Green-Ruiz, Y., Hagen, E., Kawasaki, T., Lluch-Belda, D., Lluch-Cota, S. E., MacCall, A. D., Matsuura, Y., Nevárez-Martínez, M. O., Parrish, R. H., Roy, C., Serra, R., Shust, K. V., Ward, M. N., and Zuzunaga, J. Z.: Worldwide large-scale fluctuations of sardine and anchovy populations, South African Journal of Marine Science, 21, 289–347, https://doi.org/10.2989/025776199784125962, 1999.

Segura-Noguera, M., Blasco, D., and Fortuño, J.-M.: An improved energy-dispersive X-ray microanalysis method for analyzing simulta-

870 neously carbon, nitrogen, oxygen, phosphorus, sulfur, and other cation and anion concentrations in single natural marine microplankton cells, Limnology and Oceanography: Methods, 10, 666–680, https://doi.org/10.4319/lom.2012.10.666, 2012.

Segura-Noguera, M., Blasco, D., and Fortuño, J.-M.: Taxonomic and Environmental Variability in the Elemental Composition and Stoichiometry of Individual Dinoflagellate and Diatom Cells from the NW Mediterranean Sea, PLOS ONE, 11, e0154 050, https://doi.org/10.1371/journal.pone.0154050, 2016.

875 Sharp, J. H.: Improved analysis for "particulate" organic carbon and nitrogen from seawater, https://doi.org/10.4319/lo.1974.19.6.0984, 1974.

Sigman, D. M., Altabet, M. A., Francois, R., McCorkle, D. C., and Gaillard, J.-F.: The isotopic composition of diatom-bound nitrogen in Southern Ocean sediments, Paleoceanography, 14, 118–134, https://doi.org/10.1029/1998PA900018, 1999.

Stramma, L., Johnson, G. C., Sprintall, J., and Mohrholz, V.: Expanding Oxygen-Minimum Zones in the Tropical Oceans, Science, 320, 655–658, https://doi.org/10.1126/science.1153847, 2008.

880 Taucher, J., Bach, L. T., Boxhammer, T., Nauendorf, A., Achterberg, E. P., Algueró-Muñiz, M., Arístegui, J., Czerny, J., Esposito, M., Guan, W., Haunost, M., Horn, H. G., Ludwig, A., Meyer, J., Spisla, C., Sswat, M., Stange, P., and Riebesell, U.: Influence of Ocean Acidification and Deep Water Upwelling on Oligotrophic Plankton Communities in the Subtropical North Atlantic: Insights from an In situ Mesocosm Study, Frontiers in Marine Science, 4, https://doi.org/10.3389/fmars.2017.00085, 2017.

Teuber, L., Schukat, A., Hagen, W., and Auel, H.: Trophic interactions and life strategies of epi- to bathypelagic calanoid copepods in the tropical Atlantic Ocean, Journal of Plankton Research, 36, 1109–1123, https://doi.org/10.1093/plankt/fbu030, 2014.

van Guelpen, L., Markle, D. F., and Duggan, D. J.: An evaluation of accuracy, precision, and speed of several zooplankton subsampling techniques, ICES Journal of Marine Science, 40, 226–236, https://doi.org/10.1093/icesjms/40.3.226, 1982.

Walsh, J. J.: A carbon budget for overfishing off Peru, Nature, 290, 300–304, https://doi.org/10.1038/290300a0, 1981.

Ward, B. B., Kilpatrick, K. A., Renger, E. H., and Eppley, R. W.: Biological nitrogen cycling in the nitracline, Limnology and Oceanography, 34, 493–513, https://doi.org/10.4319/lo.1989.34.3.0493, 1989.

Welschmeyer, N. A.: Fluorometric analysis of chlorophyll a in the presence of chlorophyll b and pheopigments, Limnology and Oceanography, 39, 1985–1992, https://doi.org/10.4319/lo.1994.39.8.1985, 1994.

Wiebe, P. and Holland, W.: Plankton patchiness: Effects on repeated net tows, Limnology and Oceanography, 13, 315–321, https://doi.org/10.4319/lo.1968.13.2.0315, 1968.